

SYNTHESIS ROUTES FOR LARGE VOLUMES OF NANOPARTICLES

Ombretta Masala and Ram Seshadri

Materials Department and Materials Research Laboratory, University of California, Santa Barbara, California 93106; email: masala@engineering.ucsb.edu, seshadri@mrl.ucsb.edu

Key Words inorganic materials, metals, semiconductors, oxides

■ **Abstract** This review focuses on the preparation of capped nanoparticles of inorganic materials, classified by composition. The materials described include elemental metals and metalloids (semiconductors), chalcogenide II–VI and IV–VI semiconductors, III–V semiconductors, and oxides (both of simple- and multitransition metal). Although particular emphasis is placed on methods that yield large volumes of nanoparticles, recent novel methods that may not necessarily be scalable are also reviewed. The review makes apparent the richness of chemistry that has become routine to practitioners in the field; diverse inorganic systems with distinct chemistry require distinct methods of preparation.

INTRODUCTION

The possibility to prepare monodisperse inorganic nanoparticles of pure materials in the sub-20 nm size regime, associated with the capping of these particles by (typically) functionalized long-chain organic molecules, has thrown open an entire field of research. Inorganic nanoparticles are finding myriad uses, ranging from traditional ones, such as coloring agents (in stained glass windows) and catalysts, to more novel ones, such as magnetic drug delivery, hypothermic cancer therapy, contrast agents in magnetic resonance imaging, magnetic and fluorescent tags in biology, solar photovoltaics, nano bar codes, and emission control in diesel vehicles. This field is, in certain ways, reaching maturity, and to go to the next step, it is becoming important to develop methods of scaling up the synthesis of these materials.

We do not discuss the properties and uses of nanoparticles, except so far as the properties might be a part of the process of characterization. Also, this review does not concern itself with the vast literature of nanophase materials, which are monolithic materials comprising crystalline grains whose dimensions are in the nanometer range. Such materials are typically prepared using sol-gel and related techniques. This is an older, more mature area that continues to attract a

great deal of interest (1). There is growing interest in controlling the shapes of nanophase and nanoparticulate materials, as described, for example, in the chapter by Law et al. (2) on nanotubes and nanowires and that by Kolmakov & Moskovits (3) on chemical sensing by nanostructures (see this volume). We make no attempt to describe attempts to control the shapes of nanoparticles except when they are incidental to the synthesis.

Au

The usual synthetic route to prepare gold nanoparticles involves the reduction of a suitable metal salt (usually an halide) in solution in the presence of a stabilizer. The first systematic studies of this method were by Michael Faraday who obtained colloidal gold by reducing an aqueous solution of AuCl_4^- with phosphorus (4). Since then, the discovery of various reducing agents and stabilizers have made possible the development of mild conditions that can be employed for the preparation of large amounts of nanoparticles of reproducible quality. Among these reduction methods, the best known is that developed by Brust et al. (5), which involves the phase transfer of AuCl_4^- from aqueous to organic solutions followed by reduction with NaBH_4 in the presence of alkanethiols to yield gold nanoparticles in the size range of 1–3 nm. Thiols are excellent stabilizers for capping gold nanoparticles owing to strong Au-S bonding, which enables the isolation of the particles as solid materials following solvent evaporation (6). The isolated particles can be readily redissolved in nonpolar solvents where they are indefinitely stable. Other good protective agents, such as phosphanes (7), phosphines (8), amines (9), chalcogenides (10), carboxylates (11), and polymers (12, 13), have been successfully used. The size and morphology of the gold nanoparticles can be tuned by varying the concentration ratio of capping agent to metal salts (14–16) and by choosing a suitable reducing agent (13). A weak reducing agent, such as citrate (17–19) or tartarate (13), will favor a slow reaction allowing particle growth over a long period to yield faceted and small (<1 nm) nanoparticles, whereas with relatively strong reducing agents, such as formamide (20) or *o*-anisidine (21), bigger and generally spherical nanoparticles will form. Prasad et al. (22) have shown that thiol-stabilized gold colloids obtained by reduction can be subjected to a digestive ripening process that significantly reduces the average particle size and polydispersity. The ripening process (Figure 1) involves refluxing of the particles near the boiling point of the solvent (usually toluene) in the presence of an excess of stabilizer and has been successfully employed not only with thiols but also with other protective agents, such as amines, silanes, and phosphines (23).

Another method that is of great potential for the synthesis of gold nanoparticles in large quantities, owing to mild conditions and relatively nontoxic reagents, is based on the solvated metal atom dispersion (SMAD) technique. This method, first reported by Klabunde and coworkers (24, 25), involves the vaporization of gold under vacuum followed by deposition on the inside walls of the vacuum chamber cooled to liquid nitrogen temperature simultaneously with the vapors of an organic

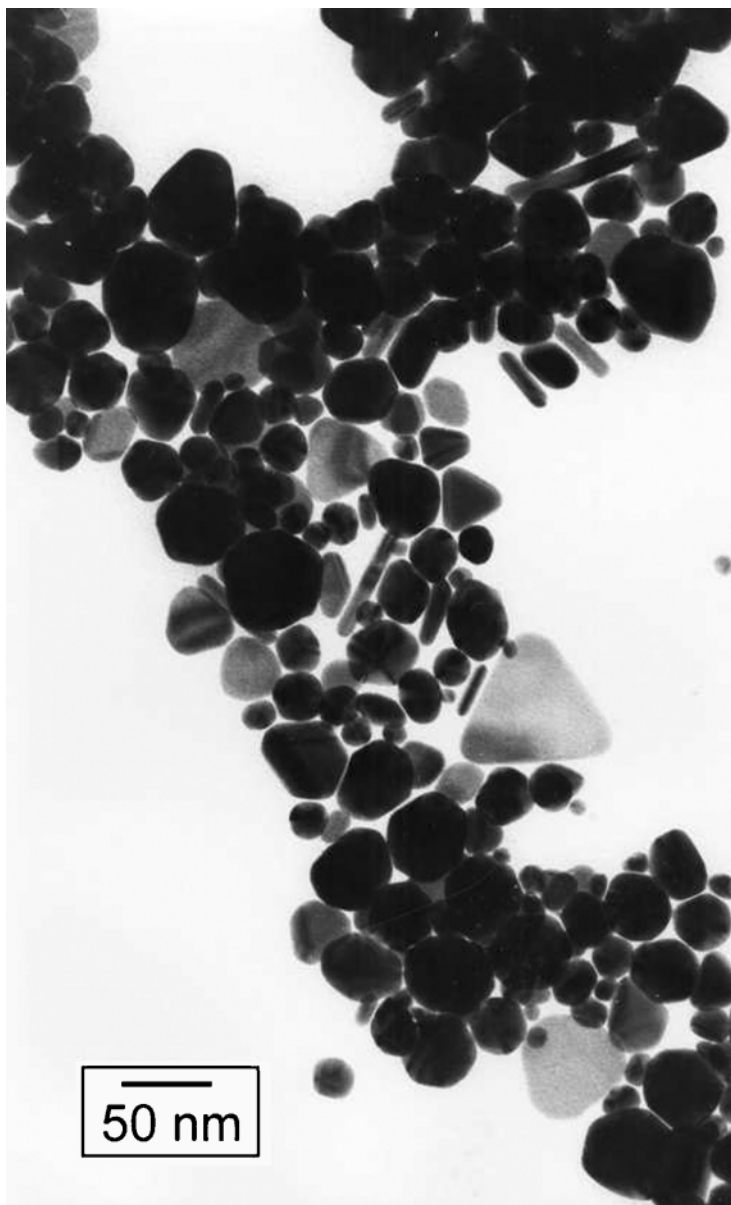


Figure 1 TEM images of (a) as-prepared gold particles and (b) the particles after addition of dodecanethiol at room temperature. These correspond to the first stages of so-called digestive ripening, which permits very narrow size distributions to be obtained. Reproduced from the work of Klabunde and coworkers (22). Reproduced with permission from the American Chemical Society.

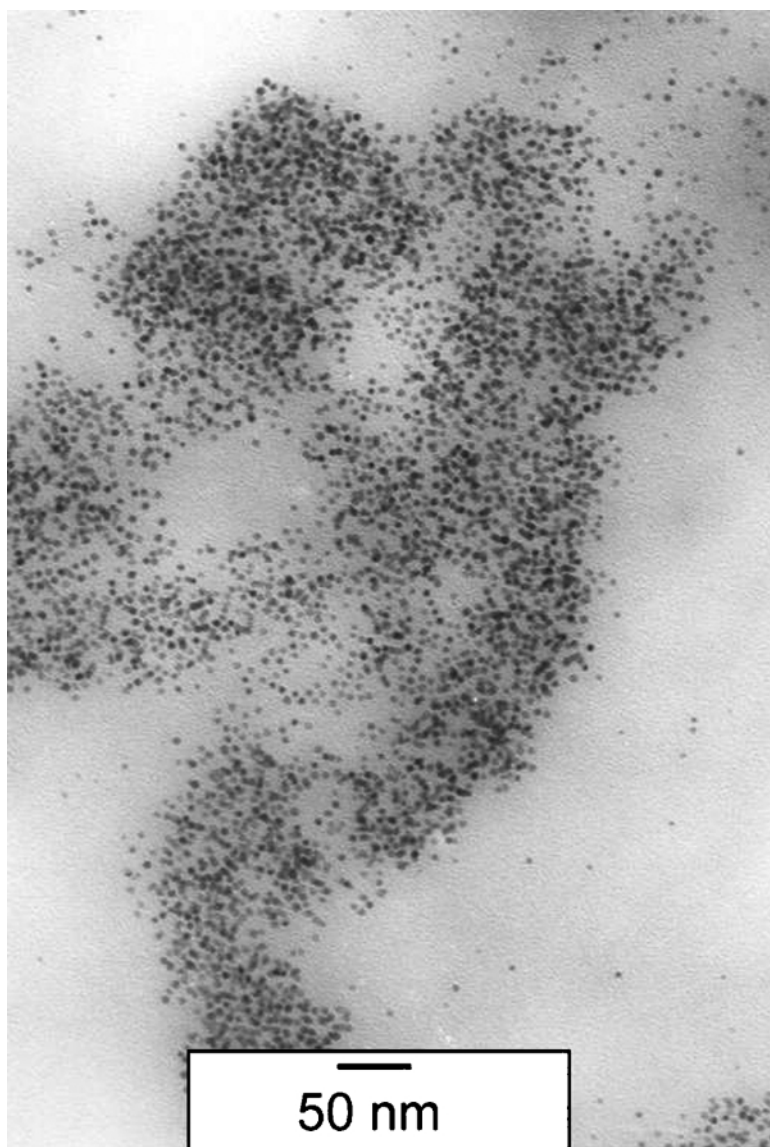


Figure 1 (Continued)

solvent, usually toluene. There are no by-products resulting from the reduction of the metal salt, and the gold colloids can be easily isolated as solid materials and redispersed in nonpolar solvents. The nanoparticles are nearly spherical in shape with sizes in the range of 1–6 nm. However, their size distribution can be further narrowed to 4–5 nm by the digestive-ripening procedure described earlier.

Ag

Nearly monodisperse silver nanoparticles can also be synthesized via reduction of a suitable salt, usually AgNO_3 or silver acetate, in solution in the presence of a stabilizer (26). As in the case of gold, many variations of this method have been developed in the past decade. NaBH_4 (14, 27, 28), sodium citrate (29), potassium bitartrate (13), dimethyl formamide (30), ascorbic acid (31), and alcohols (32, 33) are some of the reducing agents that have been successfully used. Long-chain *n*-alkanethiols are the most common protective agents employed to stabilize silver colloids (26), even though aromatic amines such as aniline (29), carboxylic acids (28, 34), and polymers (13, 33) have been also employed. However, these methods can lead to significantly different results in terms of size and morphology depending not only on the choice of the reducing agent and stabilizer but also on the reaction conditions. The synthesis of monodisperse silver nanocubes (100 nm) by reduction of silver nitrate with ethylene glycol reported by Sun & Xia (35) is noteworthy. In this preparation, ethylene glycol serves both as reducing agent and solvent, whereas *poly*(vinylpyrrolidone) is used as a capping agent. They show that by controlling experimental conditions, such as temperature, metal salt concentration, metal/stabilizer ratio, and growth time, the size and morphology of the silver nanocrystals can be easily tuned, and large quantities of highly symmetric silver nanocubes of various dimensions (from 50 to 100 nm) can be obtained (Figure 2).

Recently, a new procedure for the preparation of highly monodisperse myristate-capped silver nanoparticles has been reported (36). This method involves the suspension of silver myristate in triethylamine followed by gentle heating at 80°C for 2 h, which gradually produces a solution of uniformly spherical silver nanoparticles that can be precipitated by addition of acetone. Thus, the nanoparticles can be isolated as solid materials and redispersed in nonpolar solvents where they are stable for up to 1 week. The particle size and size distribution are affected by the alkyl chain length of the carboxylate ligand and the tertiary amine. For example, with silver stearate the particles are highly monodispersed with sizes between 1.9–3.5 nm, whereas with silver octanoate the particle distribution is broad and the sizes are larger (between 5.5 and 31.5 nm). With octylamine in the place of triethylamine, the particle size decreases, but the size distribution is also broader. This procedure is of a great promise for scale-up because of the ease of preparation, mild conditions, and use of relatively nontoxic reagents.

Pd AND Pt

The usual technique for the synthesis of palladium and platinum nanoparticles is the chemical reduction of the metal salt, usually a chloride, in the presence of a stabilizer. A variety of reducing agents have been successfully employed, including NaBH_4 (37–41), potassium bitartrate (13), superhydrides (42), amines, and alcohols (33, 43, 44). The most common capping agents are *n*-alkanethiols

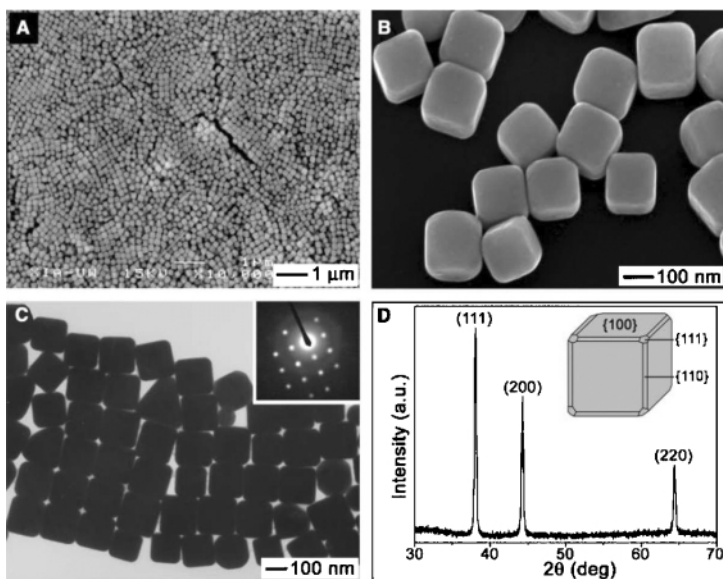


Figure 2 (A, B) SEM and (C) TEM images of silver nanocubes. (D) X-ray diffraction pattern of silver nanocubes. The inset in (D) is a scheme of the nanocube morphology. Reproduced from Sun and Xia (35). Reproduced with permission from the American Association for the Advancement of Science.

and polymers, but a few examples of Pt and Pd nanoparticles capped with amines (45), alkyl isocyanides (46), and cyclodextrins (47) have also been reported.

Very recently, Kim et al. (48) developed a new synthetic method for palladium nanoparticles involving the thermal decomposition at 300°C of a solution of the metal acetate in a surfactant. With tri-*n*-octylphosphine (TOP) and a mixture of TOP/oleylamine as surfactants, highly monodisperse palladium nanocrystals of sizes of 3, 5, and 7 nm were obtained depending on the surfactant mole ratio. With only oleylamine as surfactant, polydisperse nanoparticles with an average size larger than 10 nm were produced. The quality of the as-synthesized nanoparticles, the ease of preparation, and the fact that no further size-selective technique is required make this the first method that can be easily adapted for large-scale production of palladium nanoparticles.

Co, Ni, Fe, AND Cu

Although significant progress has been achieved in the synthesis of monodisperse noble metal nanoparticles, synthetic routes for magnetic Fe, Co, and Ni nanoparticles have yet to be improved (49). Synthesis in inverse micelles and sonochemical

decomposition of the metal carbonyls have been reported for the preparation of nanosized colloids of Co (50, 51), Fe (52–54), and Ni (55), but these methods yield, in most cases, polydisperse particles and are perhaps not suitable for scale up because of the difficulty of reproducibility at high volumes and high concentrations. However, a few synthetic procedures that are of great promise for the synthesis of monodisperse magnetic nanoparticles have been reported. For example, Co nanoparticles can be prepared with a method developed by Murray and coworkers, which involves the reduction of Co chloride by a superhydride in solution in the presence of a stabilizer, usually a mixture of oleic acid and an alkylphosphine (56, 57). The average particle size can be tuned by carefully selecting the type of alkylphosphines employed in conjunction with oleic acid because the steric hindrance of the alkyl groups can exert a control on the rate of particle growth. Thus, bulky long-chain phosphines such as TOP will tend to inhibit the growth and favor small particles (2–6 nm), whereas shorter-chain and less bulky phosphines such as tributylphosphine will permit growth and lead to bigger particles (7–11 nm). The as-synthesized nanoparticles are surrounded by a robust organic shell and can be readily dispersed in aliphatic, aromatic, and chlorinated solvents, reprecipitated by short-chain alcohols, which further reduce the size by selective precipitation. Fatty acids other than oleic acid, such as octanoic and dodecanoic acids, can be used to cap the particles through a simple ligand exchange process even though acids with an alkyl chain shorter than C8 are not strong enough to stabilize the particles. Reduction of metal acetates in solution by polyalcohols or NaBH₄ in the presence of stabilizers (oleic acid, TOP, tributylamine, and hexadecylamine have been employed) is also a successful route to synthesize highly monodisperse Co, Ni, and Ni-Co nanoparticles (58, 59).

A new approach for the synthesis of Co nanoparticles has been developed by Dinega & Bawendi (60) based on the thermal decomposition (200°C) of dicobalt-octacarbonyl, Co₂(CO)₈, in the presence of tri-*n*-octylphosphine oxide (TOPO) as a surfactant to yield rather polydisperse nanocrystals with an average diameter of 20 nm. One advantage of this method compared with the reduction synthesis described above is the absence of by-products because CO is released and elemental Co is the only nonvolatile product left in the reaction vessel. Recently, variations (61–65) of this method have been reported where monodisperse Co nanocrystals with tunable sizes between 3–20 nm can be obtained by using a combination of carboxylic acids, amines, and phosphines as surfactants, and separation of the nanocrystals from solution is achieved by magnetically induced precipitation rather than by addition of a polar solvent. This method can be also adapted for the synthesis of uniform Fe nanoparticles by replacing Co₂(CO)₈ with Fe(CO)₅ at higher temperatures (58, 66); for the synthesis of bimetallic Fe-Co (58) and Fe-Mo (67) nanoparticles by thermal decomposition of a mixture of the corresponding metal carbonyls; for Fe-Pt (68), Co-Pt (69, 70), and Fe-Pd (70) nanoparticles by simultaneous decomposition of, respectively, Fe(CO)₅ or Co₂(CO)₈ and reduction of platinum or palladium acetonate. Another organometallic precursor, Co(η^3 -C₈H₁₃)(η^4 -C₈H₁₂), has been successfully employed to prepare small Co

nanoparticles (average size 1 nm) by thermal decomposition in the presence of *poly*(vinylpyrrolidone) as a stabilizing agent (71).

Very little work has been carried out on Cu nanoparticles. Some attempts have been made to synthesize Cu nanoparticles by chemical reduction in solution (72, 73) and reduction in reverse micelles (74); however, these methods yielded particles of irregular shapes and wide size distributions. High-quality Cu nanoparticles were recently produced via an organometallic route using the CVD precursor $\text{Cu}[\text{OCH}(\text{CH}_3)\text{CH}_2\text{N}(\text{CH}_3)_2]$ (75). When the thermal decomposition of the precursor was carried out at 300°C in hexadecylamine as a hot coordinating solvent, uniform spherical particles of 7.5 nm formed. In the presence of TOPO, the decomposition yielded bigger particles with different shapes (oval, spherical, and elongated) and sizes (8–100 nm), with the elongated ones predominating at high precursor concentration. Thus the synthesis procedure can be controlled by tailoring reaction parameters such as temperature, nature of the capping agent, and precursor concentration.

Si AND Ge

Unlike II–VI and III–V semiconductors, the synthesis of group IV semiconductors silicon and germanium has not been extensively studied; however, interest in these materials has grown rapidly in the past decade owing to a number of studies suggesting that luminescence in porous silicon and silicon nanoparticles may be caused by quantum confinement (76–78). Despite a great deal of experimental and theoretical work, the origin of luminescence in silicon and its dependence on the nanoparticle size are still controversial. Some groups have observed clear changes in the wavelengths and intensities of luminescence with varying sizes or with modification of particle surface (79–81), whereas others have reported evidence to the contrary (82). Understanding the luminescent properties of silicon nanoparticles is of extreme importance for the application of these materials in the electronics industry, in particular as components in optoelectronic devices. Belonging to the same group, and therefore having semiconducting properties similar to silicon, germanium nanocrystals are also expected to show optical properties related to quantum confinement, and evidence of this has been provided (83–85).

Early work by Brus and coworkers (78, 81, 86–88) on the preparation of silicon nanoparticles from the gas phase, while not important from the viewpoint of scale-up, represents the first step toward the study of the photophysics of these materials. The preparation involves a three-step procedure carried out in a quartz reactor with a flowing system: First, a mixture of disilane-helium is flowed at a controlled rate into the pyrolysis chamber at 1000°C and 1 atm, followed by immediate dilution into a O_2 -He mixture and decrease of temperature to 200°C–300°C to stop growth and aggregation. The particles are finally collected in a solution of ethylene glycol to yield a robust colloid that is stable under air without signs of flocculation over several months. The resulting surface-oxidized nanoparticles

are crystalline, present weak luminescence emission at room temperature, and their sizes (ranging between 3 and 8 nm) can be tailored by controlling the flow rate and the initial disilane concentration because the average particle size decreases with decreasing flow rate and decreasing concentration. The nanocrystals can be efficiently separated by size-selective precipitation and by size-exclusion chromatography techniques, which prove to be very valuable in the study of the quantum confinement of luminescence (86, 88).

CO₂-laser-induced decomposition of SiH₄ in a gas flow reactor has been shown to be very useful for the synthesis of large quantities of silicon nanoparticles (89–95). In a typical reaction set-up, SiH₄ in an inert gas is exposed to focused radiation from a pulsed CO₂ laser in the reaction chamber resulting in the dissociation of the silane molecules by resonant laser absorption. The growth of the so-formed silicon nuclei is abruptly stopped as soon as they leave the hot chamber, and they are subsequently extracted from an adjacent high-vacuum chamber through a conical nozzle. The resulting nanoparticles have sizes that can be tuned in the 3–20 nm range by varying the silane concentration and flow rate and are characterized by strong visible luminescence. The particles are extremely pure because the reactor walls remain cold and therefore unreactive during the pyrolysis process. One of the main advantages of this method is that production of large amounts of powders (20–5000 mg/h) can be easily achieved by improving the flow reactor capabilities (89, 95).

The first example of a solution route to Si nanocrystals was developed by Heath (96) more than a decade ago and involves the reduction of SiCl₄ and RSiCl₃ (R=H, octyl) by sodium metal in a nonpolar organic solvent at high temperatures (385°C) and high pressures (>100 atm) to yield R-capped, hexagonal-shaped silicon nanoparticles. The octyl group is a more effective capping agent in terms of size control because nanoparticles with sizes ranging from 3 to 7 nm are formed, as opposed to single crystals ranging from 5 to 3000 nm obtained with R=H. On the other hand, infrared spectroscopy showed that the octyl groups are spontaneously replaced to give nanoparticles with a surface characterized by a mixture of Si–O, Si–H, and Si–Cl bonds. When the same reaction scheme is applied to germanium (R=phenyl), nanowires of 7–10 nm in diameter and up to 10 μ in length are obtained (97). Reduction of germanium salts was also achieved with NaK (99) and with lithium naphthalide (98). With NaK, the resulting nanoparticles are polydispersed (with sizes ranging between 8 and 20 nm), crystalline platelets, capped by a layer of GeO₂ with traces of Ge–Cl termination on the surface, and are insoluble in most polar and nonpolar solvents. With lithium naphthalide, annealing with a red laser is required to obtain crystalline nanoparticles. Following the route discovered by Heath (96), Kauzlarich and coworkers (98–108) explored the synthesis of silicon and germanium nanoparticles from reactions involving alkyl semiconductor halides or metal silicides/germanides in solution to find less extreme conditions, higher yields, and better surface manipulation, which are necessary requirements for the production of nanoparticles on a large scale. Reduction of SiCl₄ was successfully carried out at room temperature with sodium naphthalide

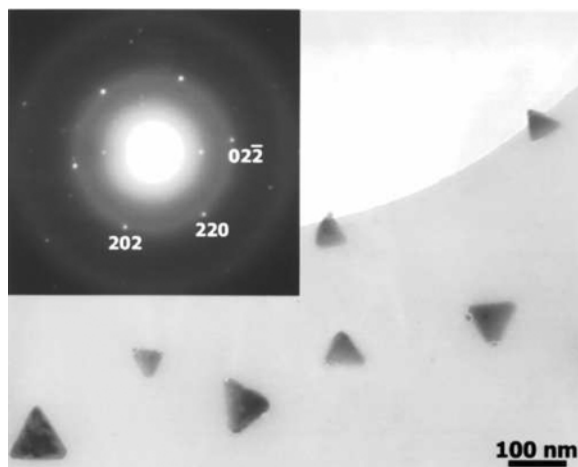


Figure 3 TEM image of alkyl-capped Si nanoparticles formed by the reduction of SiCl_4 by sodium naphthalenide in 1,2-dimethoxyethane. The surface has been capped with an excess of *n*-butyllithium. The inset shows a selected area diffraction pattern of diamond-Si. Reproduced from Baldwin et al. (104). Reproduced with permission from the American Chemical Society.

in 1,2-dimethoxyethane to give uniform, crystalline, halide-capped nanoparticles whose surface can be easily modified (103, 104) (Figure 3). For example, further treatment with an excess of octanol or *n*-butyllithium yielded, respectively, octanoxide- and *n*-butyl-capped nanocrystals. The reaction of SiCl_4 with metal silicides such as KSi , Mg_2Si , and NaSi has proved to be of great potential for the synthesis of large quantities of luminescent silicon nanoparticles with a functionalized surface. It involves refluxing the metal silicide in a suitable solvent (usually ethylene glycol dimethyl ether) under inert atmosphere in the presence of SiCl_4 followed by passivation with an appropriate capping agent (100–102). Methyl lithium, *n*-butyllithium, and several Grignard reagents have been used for the passivation step to yield alkyl-capped nanoparticles. The resulting nanoparticles showed no evidence of surface contamination from a layer of silicon oxide (a common problem in many synthetic preparations), but they presented a wide size distribution (small particles of mostly 1–5 nm were observed together with bigger particles up to 30 nm) and poor crystallinity. This method has also been employed for the synthesis of gram-quantities of organic-capped germanium nanoparticles (108–110). As in the case of silicon, the as-synthesized germanium nanoparticles are characterized by a certain degree of polydispersity, with sizes ranging from 2 to 15 nm, weak visible luminescence, but good surface stability. The formation of a layer of GeO_2 over time was observed only with the 6-(tetrahydropyranyloxy)-hexyl group as a capping agent (110). Recently, the same authors reported a variation of this method consisting in the oxidation of the metal silicide with Br_2 followed by

passivation with LiAlH_4 , butyllithium, or a Grignard reagent to give luminescent nanoparticles with a relatively high polydispersity (1–20 nm) (105–107). Work from the Kuzlarich group referred to above has definitely introduced novel routes for the synthesis of organic-capped silicon nanoparticles in solution by exploiting moderate reaction conditions, and these routes can possibly be adopted for production on a large scale. Improvements, especially in terms of size control, high yield, and crystallinity are, however, still called for.

Another solution route to monodisperse, alkyl-passivated silicon nanoparticles involves the decomposition of an organosilane precursor, such as diphenylsilane, in solvents heated and pressurized well above their critical points to temperatures between 400°C – 500°C and pressures above 80 bar (111–113). Octanol-, octene-, and octanethiol-capped silicon nanocrystals prepared by using supercritical organic solvents, such as hexane and cyclohexane, have sizes that can be tuned in the range of 1.5–3.5 nm with a narrow size distribution and are very stable to surface oxidation upon exposure in air. They also luminesce strongly at room temperature. The process should lend itself for scale-up.

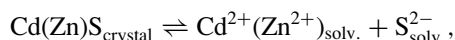
Silicon and germanium nanoparticles on a small scale can also be prepared by laser ablation (114–119) and ultrasonic methods (120–123). In the laser ablation technique, the nanoparticles are generated by irradiation of a solid target of the semiconductor metal by a focused laser beam in a reactor chamber under inert atmosphere where temperature, pressure, and residence time can be accurately controlled, followed by deposition on a hard, cold substrate. The nanoparticles are highly monodisperse, with sizes usually ranging from 1 to 5 nm, and very pure because only the metal semiconductor and inert species are present in the system. Ultrasonic synthesis involves the electrochemical etching of a silicon wafer to form porous silicon that can be dispersed in a variety of solvents by suspension in an ultrasonic cleaning bath for a determined period of time. Like in the case of the laser ablation synthesis, the main advantage of this method is the possibility of employing high-purity semiconductor-grade substrates to avoid particle surface contamination by SiO_2 and other impurities. The obtained nanocrystals present a high degree of crystallinity but also irregular shapes and sizes (from a few nanometers to several micrometers).

II–VI SEMICONDUCTORS

The synthesis and properties of II–VI semiconductor quantum dots have been extensively investigated, and several reviews on current progress in this field have been recently published (124–127). A wide range of synthetic routes have been developed for these materials, and in this section, only those methods that lend themselves to the production of nanoparticles on a large scale will be discussed. Methods for IV–VI semiconductors (notably chalcogenides of Pb) are also discussed.

Some of the earliest methods for the preparation of II–VI quantum dots date back to 1984 when Brus and coworkers (128) suggested that the optical properties of the

bulk material differ significantly from those of the same material in the nanometer size. They prepared uncapped and polymer-capped CdS (129, 130) and ZnS (130) nanoparticles (in the 3–6 nm range) by an arrested precipitation technique at room temperature involving the slow injection of the metal salt into a solution of ammonium or sodium sulfide in a suitable solvent (acetonitrile, methanol, or water). The success of the method relies on the ability to stop the crystal growth process immediately after nucleation begins by controlling the equilibrium between solid CdS (ZnS) and solvated metal ions in solution,



and this can be achieved by selecting an appropriate reaction temperature or an appropriate solvent. Weller and his group extended this technique to other semiconductor materials, such as CdSe (131), HgTe (132), and (Cd,Hg)Te (133), and to a number of capping agents, such as phosphates, amines, and especially thioalcohols (134–136). The as-synthesized thiol-capped quantum dots can be prepared on a gram scale (up to 10 g can be prepared from one synthesis reaction) as stable powders that are readily redispersed in water and possess high luminescence quantum yields (up to 50%) and high photostability. The main disadvantages of the controlled precipitation methods are that the nanocrystals present a poor degree of crystallinity, with surface defects essentially owing to the low temperatures employed, and post-treatments such as size-selective precipitation are required to obtain narrow size distributions.

Wang et al. (137, 138) proposed a simple solution synthesis for pure quantum dots of the M chalcogenides (M = Bi, Cu, Cd, Sn, Zn; chalcogenide = S, Se) that involves the reduction of S or Se in the presence of KBH_4 and the corresponding metal salt at room temperature in an appropriate solvent. The latter significantly influences the quality of the final product, yielding small uniform nanoparticles (4–6 nm) in the case of ethylenediamine and a mixed metal/chalcogenide precipitate with poor crystallinity and low yield in the case of pyridine. The role of KBH_4 is probably to reduce S to S^{2-} and Se to Se^{2-} , which react subsequently with the metal salt. Recently, amine-capped PbSe nanoparticles of tunable sizes and shapes were also obtained with this method (139). Like in the previous methods, the main limitation is the difficulty to achieve narrow size distributions and high crystallinity.

Another interesting room temperature solution synthesis that can be implemented for large-scale production involves the application of ultrasound on chemical reactions (140–142). Ultrasound irradiation results in acoustic cavitation through the formation, growth, and then implosive collapse of bubbles in a liquid. The collapse generates localized hot spots where high temperatures and pressures develop. For example, the preparation of spherical ZnSe nanoparticles of average sizes of 3, 4, and 5 nm has been achieved by mixing $\text{Zn}(\text{Ac})_2$ and selenourea in water followed by sonication with an high-intensity ultrasonic probe under inert atmosphere for a determined period of time (142). Pb and Cu selenide nanoparticles can be also obtained by using the corresponding acetates. By combining

ultrasonic irradiation with an electrochemical pulse, CdSe (140) and PbSe (141) nanoparticles with average sizes of 4 and 12 nm, respectively, have been synthesized. Parameters such as temperature, sonication time, and intensity influence the particle size, with small nanocrystals generally forming at low values. Owing to the simple reaction set-up and moderate reaction conditions, this process could be easily scaled up to form large quantities of small semiconductor nanoparticles.

The decomposition of molecular precursors at high temperatures in a coordinating solvent is, without doubt, one of the most successful routes to prepare high-quality semiconductor quantum dots. Famously, this technique was developed in 1993 by Bawendi and coworkers (143) who prepared CdE nanoparticles (E = Se, S, and Te) through separate, rapid injections of a solution of $(\text{CH}_3)_2\text{Cd}$ in TOP and a solution of TOP and the corresponding chalcogenide into TOPO at high temperatures ($\sim 200^\circ\text{C}$ – 300°C). Bis(trimethylsilyl)- and bis(*tert*-butyldimethylsilyl) salts were also employed as a source of the chalcogenide. Other than allowing particle solubility in organic solvents, the capping agent plays a crucial role in preventing particle aggregation and electronically passivating the semiconductor surface. The TOPO-Cd interaction at the surface is relatively weak so that TOPO can be easily displaced by dissolution in other solvents such as pyridine (144). The size of the nanocrystals can be easily tuned by controlling the reaction temperature with larger particles forming at higher temperatures. Many variations of this method have since been exploited. In particular, Alivisatos and his group carried out extensive studies on the CdSe system (145–147), demonstrating that parameters such as temperature, monomer concentration, and growth rate significantly influence particle size and morphology. Spherical quantum dots are usually favored at low monomer concentration and slow growth rate, whereas rod-, teardrop-, and tetrapod-like shaped nanoparticles are formed at increased growth rate [achieved by the addition of a stronger coordinating solvent than TOPO like, for example, hexyl-phosphonic acid (HPA)] and at higher monomer concentrations. Multiple injections of reagents during material growth also control the size of these nanostructures with higher injection volumes favoring, for example, longer nanorods with higher aspect ratio. A similar approach has been also used for the preparation of ZnS and ZnSe nanoparticles, CdSe/ZnS, CdSe/CdS, and CdSe/ZnSe core/shell nanostructures (148–151). The atoms in the nanocrystal surface are not fully coordinated and give rise to gap surface states and defects unless passivated. Passivation with an organic layer governs the quantum dot surface chemistry and improves optical properties, such as the emission efficiency (134). However, inorganic passivation with a semiconductor of higher band gap provides an excellent alternative not only to improve quantum efficiencies but also to decrease fluorescence lifetimes, and it confers greater stability to further treatments such as the incorporation of nanoparticles into solid structures. Also, core/shell nanoparticles exhibit novel properties that make them very attractive as a new nanocrystal system on their own (152, 153). The so-called TOPO method permits the production of highly monodisperse nanoparticles in quantities of hundreds of milligrams in one single experiment. However a great hindrance for its development on a large scale is represented by the high

temperatures employed and by the toxicity of the starting materials. In particular, alkyl metals such as $(\text{CH}_3)_2\text{Cd}$ and $(\text{CH}_3)_2\text{Zn}$ are pyrophoric, explosive at high temperatures, and liberate highly toxic gases of metal oxide so that all the reactions involving these chemicals must be carried out with extreme precautions under an inert atmosphere. In order to achieve milder and more versatile reaction conditions, many groups have attempted alternative synthetic routes.

Peng and coworkers have carried out remarkable studies in the effort to adapt the TOPO method to more stable and less toxic cadmium sources (127, 154–157). A series of experiments led to the conclusion that $(\text{CH}_3)_2\text{Cd}$ decomposes in pure hot TOPO soon after injection, producing insoluble metallic cadmium (156). In the presence of TOPO and HPA, $(\text{CH}_3)_2\text{Cd}$ is stabilized via the formation of a HPA–Cd complex that can be purified and employed to generate CdSe quantum dots of quality comparable to those described by Bawendi and coworkers, suggesting that $(\text{CH}_3)_2\text{Cd}$ is not a necessary raw material and can be replaced by other cadmium salts capable of generating the same type of complex in solution. CdO (154, 157) and cadmium salts with an anion of a weak acid, such as $\text{Cd}(\text{Ac})_2$ and CdCO_3 (155), proved to be excellent substitutes. A typical reaction involves the dissolution of the metal salt in a mixture of TOPO and another solvent (HPA, tetradecylphosphonic acid, fatty acids such as stearic acid and lauric acid, and amines such as *n*-dodecylamine have been successfully employed) at 300°C or below, followed by the addition of a solution of the chalcogenide (Se, S, or Te) in TOP. Compared to the highly unstable alkylcadmium, these salts enable a slow initial nucleation in solution with the advantages that (a) the injection temperature can be much lower and contained between 220°C–300°C; (b) both nucleation and growth are almost independent on injection conferring great reproducibility; and (c) this slow nucleation means that the initial injection can be completed within a longer time, and thus large amounts of stock solutions can be added to the reaction vessel, making the process more feasible for scale-up productions. Particle morphology can be controlled by monomer concentration, the growth temperature, and repetitive injections of the chalcogenide solution to obtain a variety of shapes from dots to rods and tetrapods, over a range of conditions (154, 157, 158) (Figure 4). The nanoparticles are monodisperse, with sizes ranging from of 2 to 25 nm and with luminescence efficiencies of up to 85% (127). This method, even though at the present time is applicable only to cadmium chalcogenides, has a great potential for scale-up production of high-quality quantum dots.

Another alternative to the use of alkylmetals for the synthesis of chalcogenide nanoparticles involves the use of single-source precursors, i.e., compounds containing both the semiconductor metal and the chalcogenide atoms already bound together in a single molecule. This method was reported earlier by Brennan et al. (159) for the preparation of CdSe nanoclusters in 4-ethylpyridine from $\text{Cd}[\text{Se}(\text{C}_2\text{H}_5)]_2$ and then extensively investigated by O'Brien and coworkers for the synthesis of ME (M = Cd, Zn, Pb; E = Se, S) quantum dots and related core/shell composites from bis(dialkyldithio-/diseleno-carbamato)metal(II) salts (160, 161). The synthesis involves the dissolution of the precursor in TOP followed by decomposition in a suitable high-boiling coordinating solvent (TOPO or 4-ethylpyridine)

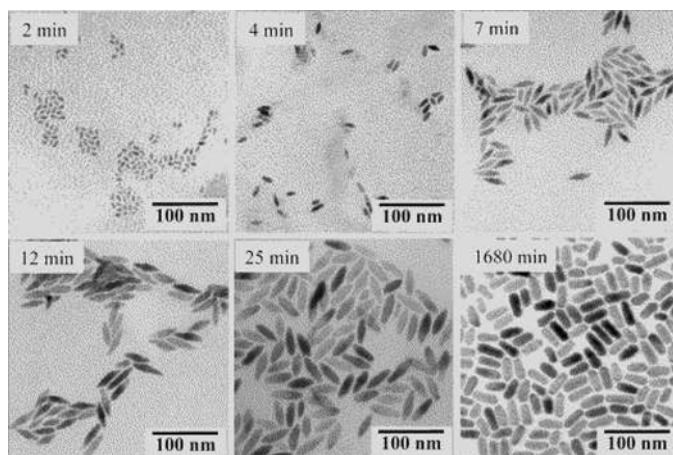


Figure 4 TEM images of the time evolution of rice-shape CdSe nanocrystals. The times are indicated. Reproduced from Peng & Peng (154). Reproduced with permission from the American Chemical Society.

usually at temperatures above 200°C. The size of the as-synthesized nanoparticles depends on the reaction time and temperature, precursor/capping agent ratio, and alkyl groups. For example, in the case of zinc, symmetrical or unsymmetrical alkyl groups lead to good quality ZnS (162) and ZnSe (163) quantum dots, whereas in the case of CdSe (164–167) and PbSe (168, 169), mainly precursors with unsymmetrical groups produce high-quality nanoparticles. In the case of CdS, by varying the growth temperature and the concentration of the precursor $\text{Cd}[\text{Se}(\text{C}_2\text{H}_5)_2]_2$, a range of morphologies from monorod, birod, tripod, tetrapod to the pencil-type rod can be easily obtained (170). The synthesis of the precursor is a simple, two-step procedure that requires first the preparation of the (dialkyldithio-/diseleno-carbamato)dialkylammonium salt by treating CSe_2 or CS_2 with an excess of amine or NaOH at 0°C, followed by reaction with an aqueous solution of cadmium or zinc chloride to yield a precipitate that is stable under aerobic conditions (171). Other single-source precursors include nitrogen-based compounds (172–174), ethylxanthate salts (175), and molecular inorganic clusters of formula $(\text{X})_4[\text{M}_{10}\text{Se}_4(\text{SPh})_{16}]$ ($\text{X} = \text{Li}, (\text{CH}_3)_3\text{NH}$). These clusters, discovered several years ago (176), have been recently employed by Cumberland et al. (177) for the synthesis of CdSe and CdSe/ZnS nanoparticles in hexadecylamine as a capping agent. By selecting the decomposition temperature of the clusters, from 100°C–300°C, particle growth can be tuned to give monodisperse nanoparticles with sizes in the 2–10 nm range. Compared to the TOPO method, the single-source precursor technique has the advantages that the syntheses for both the precursor and quantum dots are straightforward, do not involve extremely pyrophoric materials, and permit the production of high-quality nanoparticles on a gram scale.

To prepare crystalline nanoparticles, high temperatures, associated with the refluxing of reactants in high-boiling solvents, are often called for. There are many problems associated with such solvents, including possible toxicity, expense, and their inability to dissolve simple salts. A simple method to circumvent this problem is to use solvothermal methods, employing solvents well above their boiling points in enclosed vessels that support high autogenous pressures. Solvothermal (called hydrothermal when the solvent is water) methods are widespread in their use, particularly in the preparation of crystalline solids, including silicates and materials such as zeolites (178). An added advantage of solvothermal methods is that because they are carried out in closed containers, special inert conditions are not necessary. During the past five years, solvothermal techniques have become increasingly common for the synthesis of semiconductor nanoparticles. For chalcogenide nanoparticles, two preparation routes can be identified, i.e., one starting from the elements and one starting from a salt of the metal. A series of experiments with zinc and cadmium chalcogenides have shown that the solvent has a critical role in the reaction starting from the elements (179–181). In a typical setup, powders of metal and chalcogenide are ground together, inserted in a autoclave filled with the solvent up to 70% of the capacity, and then heated at a constant temperature for a determined period of time. With pyridine (179), at 180°C and 8 h, spherical ZnSe nanoparticles with sizes between 12 and 16 nm are obtained. With water (180), at 180°C and 24 h, ZnS and CdS nanoparticles with sizes ranging from 70 to 100 nm form. The latter constitutes an important example because water is a very desirable solvent, being harmless compared to the organic counterparts and therefore more suitable for scale-up. With ethylenediamine (181, 182), at 120°C and 6 h, a stable complex with likely composition Zn-E-ethylenediamine precipitates in the form of an orange compound (E = S, Se). Decomposition of the complex above 300°C under nitrogen or treatment with acid solutions yields the corresponding ZnE nanoparticles with a platelike morphology. Heating time is also an important factor in governing the particle size as shown for ZnS (179). Spherical nanoparticles with sizes of 3, 10, and 18 nm are obtained when the elements are heated in pyridine for 5, 10, and 24 hours, respectively.

Solvent and heating time also play an important role in the solvothermal reactions involving metal salts. Yu et al. (183, 184) synthesized uncapped CdE nanoparticles (E = S, Se, Te) from CdC₂O₄, Cd(NO₃)₂, and CdSO₄ in a range of solvents. Luminescent uncapped CdS, CdSe, and CdTe nanorods with diameters between 20–60 nm and lengths between 100 and 4800 nm are obtained from CdC₂O₄ in ethylenediamine, diethylenetriamine, and triethylenetetramine at temperatures above 120°C (183). Temperatures under 120°C favor the growth of a mixture of shorter nanorods and spherical particles. CdS nanorods can be obtained also at lower temperatures from cadmium sulfate or nitrate in polyamines; however, spherical particles with sizes ranging from 6 to 20 nm are preferred in solvents such as water, ethanol, tetrahydrofuran, butane-1,4-diol, and ethylene glycol (184). It is interesting to note that the solvent also affects the phase of the materials with pure hexagonal CdS prepared in ethanol or tetrahydrofuran and

a small amount of cubic phase present in CdS prepared in ethylenediamine or pyridine.

Recently, Seshadri and coworkers reported the first solvothermal method for the synthesis of thiol- and TOPO-capped CdSe (185) and CdS (186) nanoparticles. The synthesis involves heating the autoclave containing the cadmium source (cadmium stearate), S (Se), tetralin, and the capping agent (dodecanethiol or TOPO) in toluene at 200°. The driving force of the process is that tetralin is aromatized to naphthalene, a more stable compound, forming H₂S (H₂Se) in situ. In the presence of TOPO, monodisperse CdS nanoparticles of 4 nm are prepared with nearly 100% yield, whereas with dodecanethiol as a capping agent, CdSe nanoparticles of 3 nm in diameter are obtained. The as-synthesized nanoparticles are soluble in nonpolar solvents such as toluene, and their size distribution can be narrowed by size-selective precipitation techniques.

III–V SEMICONDUCTORS

Synthetic studies of III–V semiconductor nanoparticles are much less advanced compared to the II–VI analogues even though they possess a higher degree of covalent bonding, a less ionic lattice, and larger exciton diameters resulting in more pronounced quantum size effects in the optical spectra, which are very desirable for applications in optical devices (187). The preparation routes available for III–V semiconductor nanocrystals are usually an adaption of the syntheses developed for II–VI semiconductors. However, owing to the differences in the chemical properties, these typical procedures do not lead to the same results as in the case of the II–VI system (187–189). For example, the decomposition of organometallic precursors at high temperatures in coordinating solvents discovered by Murray et al. (143) has been extended to the synthesis of ME nanocrystals (M = In, Ga; E = As, P) by several groups (190–201). This method usually involves the reaction of a metal salt, such as GaCl₃ or InCl₃, with the corresponding tris(trimethylsilyl)pnictogen, P(SiMe₃)₃, or As(SiMe₃)₃ in a suitable solvent such as TOPO, TOP, quinoline, triglyme, and amines in the temperature range of 200°C–300°C. To obtain high-quality nanoparticles, the growth must be carried out over a long period of time (the process can take up to seven days), and annealing of the isolated particles at temperatures up to 400°C is often necessary to improve their crystallinity (193, 202). Even then, the as-synthesized nanocrystals present relatively large size distributions (with sizes usually ranging from 2 to 6 nm and deviation standard of ~20%), and further treatments, such as size-selective precipitation techniques, are required to achieve monodispersity. The poor quality of the nanoparticles is mainly because of the higher degree of covalency of the III–V semiconductor materials compared with the II–VI analogues. High covalency makes difficult the discrete nucleation step necessary to obtain monodisperse nanocrystals (187). Recently, Battaglia & Peng (203) showed that uniform and monodisperse InP and InAs nanoparticles can be synthesized in a

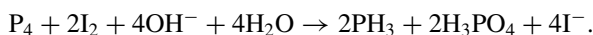
noncoordinating solvent such as octadecene in the presence of a fatty acid. The quality of the nanocrystals depends significantly on the metal:ligand ratio and the best results are observed only for a very narrow concentration window, i.e., when the ratio is 1:3. In this case, luminescent spherical nanoparticles of 3 nm in diameter and narrow size distribution ($\sim 5\%$) are obtained. Metal:ligand ratios above or below this value (1:2 or 1:4.5) result in materials with no distinguishable features in the UV-vis spectra, implying a wide size distribution. The chain length of the acid also affects the quality of the particles, with palmitic and stearic acids promoting ideal rates for particle nucleation and growth. Other than more control over particle size and morphology, this synthetic variation enables the use of a hydrocarbon as a solvent in the place of the more expensive phosphorus-based TOP or TOPO, and the process is complete within 3–4 h instead of several days.

The work of Cao & Banin (204, 205) who studied the growth of several shell structures on a core of InAs nanoparticles is worthy of note. CdSe, GaAs, InP, ZnS, and ZnSe shells can be grown on a InAs core via a two-step procedure that involves first the preparation of the InAs nanocrystals according to one of the methods described above (197) and the isolation of the particles as powders. Isolation is necessary because the size distribution is narrowed by size-selective precipitation before growing the shell. Shells of InP and GaAs can be grown only at high temperatures (240°C) by injecting a TOP solution of the corresponding metal halide XCl_3 ($\text{X} = \text{Ga}, \text{In}$) and pnictide $\text{E}(\text{SiMe}_3)_3$ ($\text{E} = \text{P}, \text{As}$) into a TOP solution of the InAs nanoparticles. For CdSe, ZnSe, and ZnS, the shell solution is prepared by mixing the alkyl metal with a TOP solution of Se [with S or $\text{S}(\text{SiMe}_3)_3$ in the case of ZnS], and injection can be achieved at temperatures as low as 150°C . In the case of InAs/InP and InAs/GaAs, a red shift in the photoluminescence spectrum is observed excluding the formation of an alloy of the two materials, and the quantum yields are significantly lowered by a factor of 8. Whereas InAs/InP nanocrystals present good solubility in organic solvents after precipitation from the growth solution, InAs/GaAs require annealing for several hours at 260°C . Formation of InAs/CdSe, InAs/ZnSe, and InAs/ZnS core/shell nanoparticles results in a red shift in the photoluminescence spectra as well, but in all cases an increase of up to 20 times in the quantum yield efficiency is reported. The quantum yield of the core/shell nanostructures increases with the shell thickness up to a threshold value beyond which further shell growth results in quenching. For ZnS and ZnSe shells, this trend can be explained considering that there is a large cell mismatch compared to InAs, and further shell growth can lead to formation of defects at the core-shell interface, resulting in carriers being trapped. In the case of CdSe, there is no lattice mismatch compared to InAs, but defects may generate at the interface because CdSe prefers to adopt the wurzite phase over the cubic one, which is typical for InAs (205).

A few examples of alternative syntheses that avoid the need of the volatile, toxic and sometimes pyrophoric silylated pnictide precursors are given in the literature. Green & O'Brien prepared luminescent, monodisperse (~ 7 nm) InP nanoparticles from the decomposition of a single-source precursor, the corresponding metal

diorganophosphide $\text{In}(\text{PBU}_2)_3$, at 167°C in 4-ethylpyridine (206). Other potential single-source precursors for GaAs and GaP nanoparticles have been synthesized by Wells et al. (202, 207). The same authors prepared relatively polydisperse GaAs and GaP nanoparticles through the in situ preparation of the corresponding pnictide $\text{E}(\text{Na/K})_3$ ($\text{E} = \text{P, As}$) in toluene followed by reflux with GaCl_3 solutions in coordinating solvents such as mono- and diglyme (208). The latter method does not involve the use of the toxic arsines or phosphines. However, the preparation of the Na/K pnictides requires the handling of hazardous and pyrophoric compounds such as Na/K alloys and elemental phosphorus or arsenic.

The synthesis of III–V semiconductor nanoparticles in aqueous solutions is hampered by the strong hydrolysis of GaX_3 and InX_3 ($\text{X} = \text{Cl, Br, I}$) and their corresponding organometallic compounds. Recently Gao et al. (209) reported the only aqueous synthesis of GaP and InP nanoparticles to date, achieved under mild conditions via a solvothermal method. The reaction involves the treatment of Ga_2O_3 or In_2O_3 with white phosphorus in the presence of I_2 in alkaline water at 120°C – 160°C for 8 h in a sealed autoclave. The role of I_2 is to induce the dismutation of phosphorus, improving the overall yield of the reaction (up to 90% for GaP):



The as-synthesized GaP and InP nanoparticles are luminescent, with a high degree of crystallinity and with an average size of 5 and 8 nm, respectively, and good monodispersity. The same authors successfully employed the GaP nanocrystals in the thermal conversion of benzene into 6-phenylfulvene (210), opening a new application field for these inorganic nanoparticles. Other solvothermal synthetic methods for the preparation of InP, InAs, and GaN have been reported by Qian et al. (211–213). Spherical InP nanoparticles of average size of 15 nm are prepared by reacting In_2Cl_3 with Na_3P in 1,2-dimethoxyethane (DME) at 180°C (211). With benzene as a solvent, the nanoparticles reach 40 nm in size. The two sizes are due to the fact that DME reacts differently from benzene, which acts only as solvent; DME is an open-chain polyether that can easily hinder the growth of the nanocrystals by forming complexes with the halide. InAs nanoparticles (average size 15 nm) are obtained with a similar reaction in xylene at 150°C in the presence of metallic zinc (212). Zinc creates a reducing environment, limiting the amount of free oxygen in the autoclave and obviating the need to perform the reaction in an inert, dry atmosphere.

OXIDES

Oxides, particularly of the transition metals, constitute a very important material class, displaying almost every known property and participating in a variety of functions (214). Because of the high oxygen content of Earth's atmosphere, oxides are also some of the most stable materials formed. Many transition metal

oxides (particularly those of the early transition metals, such as TiO_2 and ZrO_2 , and the oxides of Fe) are somewhat biocompatible, or at least, not very toxic. This is perhaps the single greatest advantage of oxide materials. Although there has been a great deal of recent work on oxide nanoparticles, the area considerably lags behind the state of the art of metal or chalcogenide nanoparticles, in part because synthesis is not as well developed and because capping is less well understood. Hyeon (49) has recently reviewed the synthesis of magnetic nanoparticles, including oxides. Rajamathi & Seshadri (215) have reviewed hydrothermal and solvothermal preparation of oxide nanoparticles, and the area itself, including synthesis, has been reviewed by one of us in a book chapter (216).

The pinnacle of synthetic sophistication in the preparation of functional oxide nanoparticles (the function being magnetism) has in fact been achieved by nature in magnetotactic bacteria. In 1975, Blakemore (217) demonstrated that certain bacteria found in marine marsh muds tended to rapidly navigate along a specific direction; the local geomagnetic North or South pole, depending on whether the bacteria habit the Northern or Southern hemisphere. In addition, Blakemore used transmission electron microscopy to demonstrate that these bacteria contained Fe-rich crystals approximately 100 nm in diameter, and Frankel et al. (218) later showed that a magnetotactic spirillum cultured in solutions containing ferric salts produced uniform single crystals of spinel Fe_3O_4 .

Microbial magnetite, as well as the ferrimagnetic sulfide biomineral greigite $\gamma\text{-Fe}_3\text{S}_4$ (found in magnetotactic bacteria that grow in marine, sulfidic environments), is an excellent example of the control that nature is able to exert over inorganic crystallization. The magnetic particles are produced to be at the optimal single domain size. Any smaller and the particles would be superparamagnetic. Any larger and the particles would develop multiple magnetic domains, making them less effective magnets. In addition, within the magnetosome, the magnetite crystals align themselves in order to provide the entire bacteria a greater restoring torque, thereby producing a very effective compass. Dunin-Borkowski et al. (219) have directly mapped the magnetism in chains of magnetite crystals in magnetotactic bacteria using transmission electron microscopy and electron holography.

As is the case for all nanoparticles, a major concern in the preparation of oxide nanoparticles is to be able to control size and shape precisely, and further, to be able to assemble the nanoparticles in ordered arrays. Biogenic magnetite provides great inspiration, suggesting what laboratory preparations can aspire to and providing hints on how these goals could be achieved. A UK-based company called NanoMagneticsTM (<http://nanomagnetics.co.uk>) has already started the process of commercialization of biomineral-inspired magnetic nanoparticles. At the time of writing, their website states that small magnetic particles (presumably ferrite-based) can be grown in the cavities of the protein apoferritin. The nanoparticles, along with their apoferritin coatings, are then annealed into arrays, carbonizing the protein in the process, and resulting in putative high data density magnetic storage media. The particles grown are then assembled into planar arrays, and the protein shells are carbonized by heating. The company website claims to have

achieved magnetic data storage densities of exceeding 12 Gbit in⁻² in 2002 using this strategy.

Many transition metal ions, particularly those in high oxidation states (which are often the more covalent ones, such as oxides of Ti⁴⁺ or Zr⁴⁺), are easily hydrolyzed in solution according to (assuming a solvated ion)



The water molecule is decomposed in the process. Typically, basic conditions are called for. However, in the preparation of oxides of amphoteric ions, such as Al(III) or Ga(III), hydrolysis can also be performed under conditions of low pH.

It is important to recognize that such hydrolysis is not possible with many ions, particularly of the electropositive elements. Alkali, alkaline earth, and rare-earth ions, for example, are too stable in solution and too ionic for hydrolysis to take place. For example, La³⁺ has the equilibrium



shifted completely to the left only when the temperature is as high as 1000 K.

Despite these limitations, hydrolytic routes have been the mainstay of many preparations of nanoparticulate oxide materials, particularly magnetic oxides of the first-row transition metals. A large portion of the reported literature on hydrolytic routes to oxide nanoparticles concerns aqueous systems. Nonaqueous media have not been greatly explored. Aprotic solvents, where hydrolysis may be more effective, could provide promising avenues for oxide nanoparticle synthesis.

Magnetic oxide (typically ferrite spinels or γ -Fe₂O₃) nanoparticles, when dispersed at high concentrations in water or oil, form ferrofluids (220). Particle sizes in these materials are usually in the 5–15 nm range—small enough that neither magnetic nor gravitational fields should cause their precipitation. The many uses of ferrofluids in magnetic seals, bearings, dampers, etc. (220), have resulted in an extensive body of literature on the preparation and properties of dispersions of magnetic oxide nanoparticles. Many of the preparative routes involve hydrolysis. In many cases, the preparation simply involves raising the pH of a solution of metal ions taken in the correct proportion by addition of base. Sorenson et al. (221) have made detailed magnetic and Mössbauer studies of MnFe₂O₄ nanoparticles prepared by precipitation at high pH followed by digestion. Cabuil and coworkers (222) have shown in the case of the preparation of CoFe₂O₄ and γ -Fe₂O₃ particles that changing the temperature and the nature of the base allows particles of different sizes to be prepared. In addition, they have suggested methods of dispersing the particles in water though controlling Coulomb repulsion between the particles. The particles can be dispersed in oils by modifying their surfaces with long-chain surfactants. Cabuil et al. (223) have also shown that size selection of particles is possible though control of a combination of surface charge and ionic strength of the dispersing medium. Morales et al. (224) have made a careful study of γ -Fe₂O₃ nanoparticles with sizes ranging from 3 to 14 nm prepared by hydrolytic means

[and also by laser pyrolysis of $\text{Fe}(\text{CO})_5$ in solution]. They show that to account for the magnetic properties of the particles, it is necessary to use a model wherein the moments on the surface of the particle are canted.

The use of polar solvents other than water to perform hydrolysis is an exciting prospect. Ammar et al. (225) have demonstrated that glycols (specifically 1,2-propanediol) can be used as a solvent under reflux to hydrolyze a mixture of Co(II) and Fe(III) salts to obtain equiaxed particles of CoFe_2O_4 with an average diameter of 5.5 nm. A combination of Mössbauer spectroscopy, X-ray absorption near-edge structure (XANES), and magnetic measurements suggested that the particles were well ordered both in terms of being crystalline and having all Co in the divalent state. Rajamathi et al. have been able to capitalize on the unusual properties of glycols—they are sufficiently polar, they can dissolve metal salts, and they can support hydrolysis, and yet, they can dissolve long-chain surfactants such as amines—in the preparation of *n*-octylamine-capped 5 nm $\gamma\text{-Fe}_2\text{O}_3$ nanoparticles (226). The particles can be dissolved in toluene when a little excess amine is added to the solvent. The particles can be precipitated through addition of a polar solvent such as 2-propanol and then redissolved in toluene/*n*-octylamine. Diethylene glycol has also been used as a solvent by Carunto et al. (227) to prepare a number of transition metal ferrites capped by long-chain carboxylic acids.

Pileni (228, 229) has reviewed the extensive work from her group on the use of reverse micelles as nanoscale reaction chambers within which nanoparticles can be prepared. In a system of water and surfactant dispersed in oil, under suitable conditions, the water forms spherical droplets of radius R_W given by

$$R_W = \frac{3V_{aq}[\text{H}_2\text{O}]}{\sigma[\text{S}]},$$

where square brackets indicate concentration, S refers to surfactant, σ is the area per head group of the surfactant molecule, and V_{aq} is the volume of a water molecule. By controlling the water and surfactant concentration, the diameter of the water droplet can therefore be controlled. If a nanoparticle is nucleated within the water sphere, its growth is limited by the size constraint of the water droplet. Pillai & Shah (230) have utilized this route to prepare high-coercivity CoFe_2O_4 nanoparticles by mixing two water-in-oil microemulsions, one containing metal ions and the other containing base. These authors calcine the particles so the resulting material is nanophase rather than nanoparticulate. MnFe_2O_4 (231) and CoCrFeO_4 (232) have been prepared using such reverse-micelle routes by Vestal & Zheng and characterized by using a combination of magnetization studies and powder neutron diffraction.

Pileni has also pioneered the use of the surfactant-as-reactant approach in the preparation of nanoparticles. For example, in the preparation of CoFe_2O_4 nanoparticles with sizes between 2 to 5 nm, instead of preparing inverse-micellar dispersions of the Co and Fe salts, Moumen & Pileni (233–235) prepared the dodecyl-sulfonate (DS) analogs $\text{Fe}(\text{DS})_2$ and $\text{Co}(\text{DS})_2$. These were made to form micellar solutions; to raise the pH, aqueous methylamine solution was added. Stirring for

two hours resulted in a magnetic precipitate. Owing to the low yield of Fe(II) to Fe(III) oxidation under these conditions, an excess of $\text{Fe}(\text{DS})_2$ is required.

With an increase in concentration of the reactants, there is an increase in particle size. Zinc-doped Co ferrite nanoparticles (236) and zinc ferrite (237) have also been prepared using these methods. The 10-nm ferrite nanocrystal ferrofluids prepared using the $\text{Fe}(\text{DS})_2$ route form deposits with different morphologies when evaporated on oriented graphite substrates (238). The morphology can be strongly influenced by applying a magnetic field during the evaporation process. Thus, magnetic properties of deposits prepared in the presence and absence of a field are quite different.

Hydrolysis can be assisted by irradiation of the reacting bath with ultrasound. In these sonochemical preparations, acoustic cavitation results in the production of concentrated spots of extremely high temperatures. These hot spots accelerate the rate of metal ion hydrolysis. Gedanken and coworkers (239) have prepared ZnO, CuO, Co_3O_4 , and Fe_3O_4 particles by subjecting solutions of the acetates to ultrasound irradiation using a high-intensity horn. Particle morphologies could be altered by using mixtures of water and dimethyl formamide instead of pure water as the solvent. Magnetite nanorods have been prepared by these authors (240) by ultrasonic irradiation Fe(II) acetate in water in the presence of β -cyclodextrin. The authors suggest that cyclodextrin molecules are acting as size-stabilizing agents.

Oxides, unlike the other chalcogenides (sulfides, selenides, tellurides) are not associated with an oxide ion source in solution. However, it is possible to directly oxidize a metal source in solution. A popular route to this is to use zero-valent carbonyls, for example, $\text{Fe}(\text{CO})_5$. Decomposing these carbonyls in solvents results in very finely divided metal particles that are easily susceptible to oxidation. In fact, exposing them to an atmosphere of air is usually sufficient to convert the particles to oxides.

Bentzon et al. (241) have prepared Fe oxide nanoparticles by decomposing $\text{Fe}(\text{CO})_5$ in decalin in the presence of oleic acid as the stabilizing ligand. Aging the ferrofluid formed in air for several weeks results in a mixture of hematite and spinel phases. This is among the first reports of nanocrystal superlattice formations. Hyeon et al. (242) have prepared monodisperse γ - Fe_2O_3 nanoparticles in the size range of 4–16 nm by decomposing $\text{Fe}(\text{CO})_5$ complexes in octyl ether at 300°C in the presence of oleic acid as a capping agent (Figure 5). Oxidation of bcc-Fe to γ - Fe_2O_3 was achieved by the addition of the organic oxidant $(\text{CH}_2)_2\text{NO}$. The resulting capped oxide nanoparticles can easily be redispersed in organic solvents, such as hexane or toluene. Particle size is altered by varying the ratio of Fe to the capping agent (oleic or lauric acids). The remarkable feature of this preparation is that the as-prepared particles are sufficiently monodisperse that they form nanocrystal superlattices without the need for a size-selection process. More recently, the same group has extended their method of aging a metal surfactant complex followed by mild oxidation to produce Co ferrite spinel nanoparticles (243).

Wagner and coworkers have prepared yttrium oxide (244) and europium-doped yttrium oxide nanoparticles (245) by first reducing rare-earth salts in solution using

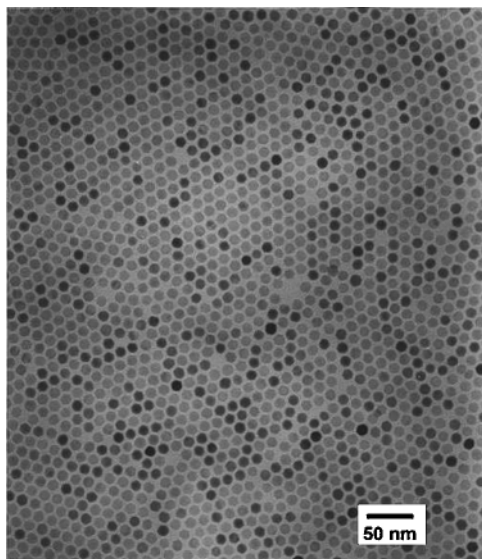


Figure 5 TEM image of monodisperse 11 nm γ - Fe_2O_3 nanoparticles prepared without size selection. Reproduced from Hyeon et al. (242). Reproduced with permission from the American Chemical Society.

alkalides (strong reducing agents that are complexes of crown ethers with alkali metals, and where the anion is a complexed electron) and then oxidizing the rare-earth metal nanoparticle so formed in aerated water. The white powders were then annealed in air. More examples of oxide nanoparticles prepared through direct oxidation are discussed along with solvothermal methods described later in the review.

If one starts with a precursor complex wherein the ligands bind to metal ions through oxygen, it could be possible to envisage a decomposition reaction that would leave behind the metal oxide. For a trivalent ion, such reactions could be generalized as



Suitable design of the R group (stable leaving groups) would ensure that the reaction proceeds in a facile manner. It should then be possible to carry out such reactions in a suitable high-temperature solvent under solvothermal conditions, possibly in the presence of a suitable capping agent.

Rockenberger et al. (246) have described the use of cupferron complexes as precursors to prepare transition metal oxide nanoparticles. Cupferron (N-phenyl, N-nitroso hydroxylamine) forms bidentate, univalent complexes with a number of different transition metal ions. These complexes easily decompose to give the oxide. The authors demonstrated the preparation of γ - Fe_2O_3 , Cu_2O , and Mn_3O_4

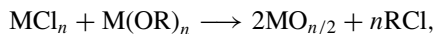
nanoparticles prepared by injecting octylamine solutions of the corresponding cupferron precursors into refluxing trioctylamine. Size is controlled by the temperature of the reaction. The particles so prepared form stable solutions in solvents such as toluene, from which they can be reprecipitated by the addition of methanol. This work is quite seminal in its generality, and particularly in the manner in which it suggests the search for suitable precursors for the preparation of oxide nanoparticles. Most importantly, it suggests thermolysis as an alternative to hydrolysis, which, as pointed out earlier, is simply not viable for a number of metal oxides.

An important contribution to the surface chemistry of metal oxide nanoparticles has been made by Rotello and coworkers (247) who have prepared γ -Fe₂O₃ nanoparticles by the cupferron decomposition method and compared the relative efficacies of different long-chain surfactants as capping agents. The most stabilizing capping agent (as monitored by ease of redissolution and stability in solution) was obtained by using a two-tailed surfactant (with 12-carbon tails) with the polar part comprising a 1,3-diol.

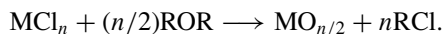
The thermolysis of Fe(III) hydroxide caprylates in boiling tetralin under argon flow gives γ -Fe₂O₄ nanoparticles (248). The surfaces of the nanoparticles could be modified by exchanging the capping caprylate groups with betaine, among other species (249). Betaine-capped γ -Fe₂O₃ nanoparticles are reported to have high solubility in water.

Using a combination of hydrolysis and oxidation, O'Brien et al. (250) have shown that the treatment of a complex alkoxide containing Ba²⁺ and Ti⁴⁺—BaTi(O₂CC₇H₁₅)[OCH(CH₃)₂]₅, an agent for the MOCVD growth of BaTiO₃—can be decomposed in diphenyl ether at 140°C in the presence of oleic acid as a capping agent to give nanocrystalline, cubic BaTiO₃. After cooling to 100°C, 30% H₂O₂ is added, and crystallization is induced over a 48 h period. Changing the ratio of capping agent to water and the amount of peroxide added permits the size of the particles to be varied. This is perhaps the only report of soluble perovskite oxide nanoparticles and, once again, is a route of great generality and interest. The authors also report using such routes to prepare PbTiO₃ and TiO₂ nanoparticles.

In a metathesis reaction, two compounds, AB and CD, exchange species to give two new compounds AC and BD. Such routes have been explored in the preparation of nanoparticles. Arnal et al. (251) have reported two nonhydrolytic routes to sol-gel metal oxides, particularly of titanium. The first route involves the reaction of a metal halide with a metal alkoxide:

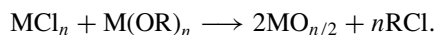


and the second route involves the reaction of a metal halide with an ether:



In both reactions, some of the driving force comes from the removal of the volatile product RCl. The first of the two methods has been employed by Colvin and coworkers (252) to prepare capped TiO₂ nanoparticles in refluxing heptadecane

with trioctyl phosphine oxide as the capping agent:

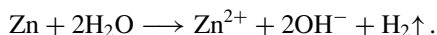


The particles formed clear solutions in nonpolar solvents, from which they could be precipitated through the addition of a polar solvent such as acetone. When trioctyl phosphine oxide was not taken with the starting materials, insoluble precipitates were obtained. Recently, a similar route has been used by Hyeon and coworkers to prepare tetragonal zirconia nanoparticles (253).

Rajamathi & Seshadri (215) have reviewed the uses of solvothermal methods for the preparation of oxide and chalcogenide nanoparticles. For oxide nanoparticles, these methods can involve hydrolysis, oxidation and thermolysis, all performed under hydrothermal or solvothermal conditions. Some of the more striking examples are provided here.

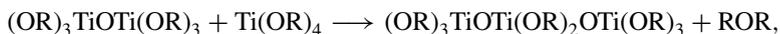
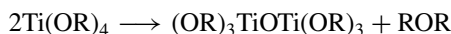
An unusual reaction reported by Inoue et al. (254) is the direct oxidation of Ce metal in 2-methoxyethanol at temperatures between 200°C and 250°C. Most of the product obtained was bulk CeO₂ as a yellow solid, but in addition, they obtained a brown solution of 2 nm CeO₂ nanoparticles. The CeO₂ nanoparticles could be salted out through the addition of NaCl and redispersed into solution at will. The solutions obeyed the Beer-Lambert law for the concentration dependence of the optical extinction, suggesting that the nanoparticulate dispersion was a genuine solution.

Starting with Zn powder and GaCl₃ in water, Qian and coworkers (255) have used the fact that the oxidation of Zn to Zn²⁺ in water is associated with the production of hydroxyl ions according to



The OH⁻ ions help in the hydrolysis of Ga³⁺ to eventually give, in the presence of Zn²⁺, the spinel ZnGa₂O₄. The authors used a 10%–20% over-stoichiometry of Zn, and the reaction was carried out at 150°C for 10 h. 10-nm ZnGa₂O₄ nanoparticles were obtained. Excess ZnCl₂ formed in the reaction could be washed away with water.

Chemseddine & Moritz (256) have used the polycondensation of titanium alkoxide Ti(OR)₄ in the presence of tetramethylammonium hydroxide to obtain highly crystalline anatase nanoparticles with different sizes and shapes. A general, step-wise reaction for such polycondensation could be written as



and so on to anatase, although it might not proceed in precisely this manner in the presence of base. The reactions were performed in two steps: First alkoxide was added to the base at 0°C in alcoholic solvents in a three-necked flask. The temperature was then raised to reflux. The second stage involved treating the product of the reflux in Ti autoclaves under a saturated vapor pressure of water

(2500 kPa) at temperatures between 175°C and 200°C for 5 h. Sufficiently monodisperse nanocrystals were obtained so that they formed coherent superlattices as monitored by low-angle powder X-ray diffraction. By using other hydroxides with bulkier alkyl groups (for example, tetrapropylammonium hydroxide) some control over crystallite morphology became possible.

Wu et al. (257) have combined microemulsion and inverse-micelle techniques with hydrothermal techniques in the preparation of rutile and anatase TiO₂ nanoparticles. They used the system water-cyclohexane-Triton X-100 with *n*-hexanol as a second emulsifier. In the water-filled micellar pockets were Ti(OR)₄ (R = butyl) acidified with HCl or HNO₃. Treating the system at 120°C–200°C for 12–144 h gave anatase particles. When high HCl concentrations were employed, rutile rods were obtained.

Hirano (258) has prepared spinel ZnGa₂O₄ nanoparticles by adjusting the pH of Zn and Ga sulphates with NH₃ to different initial values (varied from 2.5 through 10). The material was heat treated hydrothermally at temperatures between 150°C

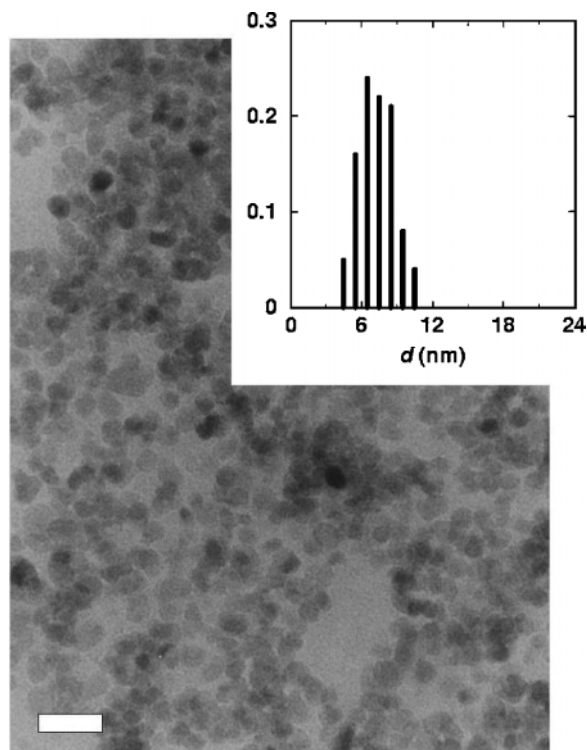


Figure 6 TEM image of 7 nm *n*-octylamine-capped CoFe₂O₄ nanoparticles prepared in solvothermal toluene. The bar is 20 nm. Reproduced from (263) with permission from the Royal Society of Chemistry.

and 240°C for times between 5 and 50 h. Particle sizes could be varied from 5 to 25 nm.

Cabañas et al. (259, 260) have described the preparation of nanoparticulate CeO₂-ZrO₂ solid solutions under flow-hydrothermal conditions, wherein the reactants are taken to the final temperature very rapidly in a continuous process. The advantage of performing hydrothermal reactions in such a manner is, first, that a large amount of material can be processed, permitting simple scale up. Second, the nucleation step can be made very rapid as a result of the rapid heating. This can help separate nucleation and growth and can thereby satisfy the famous LaMer criterion (261) for obtaining monodisperse particles. Cabañas & Poliakoff (262) have also prepared a number of spinel ferrite samples in this way, starting from mixtures of different Fe(II) and M(II) acetates (M = Co, Ni, Zn and Co/Ni). Most of the preparations yielded a bimodal distribution of sample sizes, with the smaller samples being approximately 10 nm in diameter, and the larger ones approximately 100 nm.

Recently, Thimmaiah et al. (263) have extended the thermolytic route to oxide nanoparticles devised by Rockenberger et al. (246) to solvothermal conditions. Using solvothermal toluene (typically at 220°C for 1 h), cupferron precursors of Fe, and of Co and Fe are decomposed to obtain sub-12 nm maghemite γ -Fe₂O₃ nanoparticles and spinel CoFe₂O₄ nanoparticles. The reactions do not work in the absence of long-chain amines (*n*-octylamine and *n*-dodecylamine), which are added as capping agents. A complete characterization of the magnetic properties of these nanoparticles has been presented by the authors. This is the only report to date of capped oxide nanoparticles prepared from a solvothermal route (Figure 6).

ACKNOWLEDGMENT

This work is supported by the Petroleum Research Fund of the American Chemical Society under a type AC award. We also acknowledge a start-up grant from the Dean, College of Engineering, UCSB, and thank Paul O'Brien for discussions and encouragement.

**The Annual Review of Materials Research is online at
<http://matsci.annualreviews.org>**

LITERATURE CITED

1. Gleiter H. 1989. Nanocrystalline materials. *Prog. Mater. Sci.* 33:223–315
2. Law M, Goldberger J, Yang P. 2004. Semiconductor nanowires and nanotubes. *Annu. Rev. Mater. Res.* 34:83–122
3. Kolmakov A, Moskovits M. 2004. Chemical sensing and catalysis by one-dimensional metal oxide nanostructures. *Annu. Rev. Mater. Res.* 34:151–80
4. Faraday M. 1857. Experimental relations of gold (and other metals) to light. *Phil. Trans. R. Soc. London* 147:145–81
5. Brust M, Walker M, Bethell D, Schiffrin DJ, Whyman R. 1994. Synthesis of thiol-derivatized gold nanoparticles in a 2-phase liquid-liquid system. *Chem. Commun.* 7:801–2

6. Schmid G, Corain B. 2003. Nanoparticulated gold: syntheses, structures, electronics and reactivities. *Eur. J. Inorg. Chem.* 17:3081–98
7. Schmid G, Lehnert A. 1989. The complexation of gold colloids. *Angew. Chem. Int. Ed. Engl.* 28:780–81
8. Weare WW, Reed SM, Warner MG, Hutchinson JE. 2000. Improved synthesis of small phosphine-stabilized gold nanoparticles. *J. Am. Chem. Soc.* 122:12890–91
9. Leff DV, Brandt L, Heath JR. 1996. Synthesis and characterization of hydrophobic, organically-soluble gold nanocrystals functionalized with primary amines. *Langmuir* 12:4723–30
10. Brust M, Stuhr-Hansen N, Norgaard K, Christensen JB, Nielsen LK, Bjornholm T. 2001. Langmuir-Blodgett films of alkane chalcogenide (S, Se, Te) stabilized gold nanoparticles. *Nano Lett.* 1:189–91
11. Yao H, Momozawa O, Hamatami T, Kimura K. 2001. Stepwise size-selective extraction of carboxylate-modified gold nanoparticles from an aqueous suspension into toluene with tetraoctylammonium cations. *Chem. Mater.* 13:4692–97
12. Corbier MK, Cameron NS, Sutton M, Mochrie SGJ, Lurio LB, et al. 2001. Polymer-stabilized gold nanoparticles and their incorporation into polymer matrices. *J. Am. Chem. Soc.* 123:10411–12
13. Tan Y, Dai X, Li Y, Zhu D. 2003. Preparation of gold, platinum, palladium and silver nanoparticles by the reduction of their salts with a weak reductant-potassium bitartrate. *J. Mater. Chem.* 13:1069–75
14. Heath JR, Knobler CM, Leff DV. 1997. Pressure/temperature phase diagrams and superlattices of organically functionalized metal nanocrystals monolayers: the influence of particle size, size distribution and surface passivant. *J. Phys. Chem. B* 101:189–97
15. Hostetler MJ, Wingate JE, Zhong CJ, Harris JE, Vachet RW, et al. 1998. Alkanethiolate gold cluster molecules with core diameters from 1.5 to 5.2 nm: core and monolayer properties as a function of core size. *Langmuir* 14:17–30
16. Leff DV, Ohara PC, Heath JR, Gelbart WM. 1995. Thermodynamic control of gold nanocrystal size: experiment and theory. *J. Phys. Chem.* 99:7036–41
17. Zhu T, Vasilev K, Kreiter M, Mittler S, Knoll W. 2003. Surface modification of citrate-reduced colloidal gold nanoparticles with 2-mercaptosuccinic acid. *Langmuir* 19:9518–25
18. Frens G. 1973. Controlled nucleation for regulation of particle-size in monodisperse gold suspensions. *Nat. Phys. Sci.* 241:20–22
19. Turkevich J, Stevenson PC, Hillier J. 1951. A study of the nucleation and growth processes in the synthesis of colloidal gold. *Discuss. Faraday Soc.* 11:55–75
20. Han MY, Quek CH, Huang W, Chew CH, Gan LM. 1999. A simple and effective chemical route for the preparation of uniform nonaqueous gold colloids. *Chem. Mater.* 11:1144–47
21. Dai X, Tan Y, Xu J. 2002. Formation of gold nanoparticles in the presence of *o*-anisidine and the dependence of the structure of poly(*o*-anisidine) on synthetic conditions. *Langmuir* 18:9010–16
22. Prasad BLV, Stoeva SI, Sorensen CM, Klabunde KJ. 2002. Digestive ripening of thiolate gold nanoparticles: the effect of alkyl chain length. *Langmuir* 18:7515–20
23. Prasad BLV, Stoeva SI, Sorensen CM, Klabunde KJ. 2003. Digestive-ripening agents for gold nanoparticles: alternatives to thiols. *Chem. Mater.* 15:935–42
24. Lin S, Franklin MT, Klabunde KJ. 1986. Nonaqueous colloidal gold. Clustering of metal atoms in organic media. *Langmuir* 2:259–60
25. Stoeva S, Klabunde KJ, Sorensen CM, Dragieva I. 2002. Gram-scale synthesis of monodisperse gold colloids by the solvated metal atom dispersion and digestive ripening and their organization into

- two- and three-dimensional structures. *J. Am. Chem. Soc.* 124:2305–11
26. Brust M, Kiely CJ. 2002. Some recent advances in nanostructure preparation from gold and silver nanoparticles: a short topical review. *Coll. Surf. A Phys. Eng. Asp.* 202:175–86
27. He S, Yao J, Jiang P, Shi D, Zhang H, et al. 2001. Formation of silver nanoparticles and self-assembled two-dimensional ordered superlattice. *Langmuir* 17:1571–75
28. Li X, Zhang J, Xu W, Jia H, Wang X, et al. 2003. Mercaptoacetic acid-capped silver nanoparticles colloid: formation, morphology and SERS activity. *Langmuir* 19:4285–90
29. Tan Y, Li Y, Zhu D. 2003. Preparation of silver nanocrystals in the presence of aniline. *J. Coll. Int. Sci.* 258:244–51
30. Pastoriza-Santos I, Liz-Marzan LM. 1999. Formation and stabilization of silver nanoparticles through reduction by N,N-dimethylformamide. *Langmuir* 15:948–51
31. Sondi I, Goia DV, Matijevic E. 2003. Preparation of highly concentrated stable dispersions of uniform silver nanoparticles. *J. Coll. Int. Sci.* 260:75–81
32. Lee C, Wan C, Wang Y. 2001. Synthesis of metal nanoparticles via self-regulated reduction by an alcohol surfactant. *Adv. Funct. Mater.* 11:344–47
33. Ayyappan S, Gopalan Srinivasa R, Subbanna GN, Rao CNR. 1997. Nanoparticles of Ag, Au, Pd, and Cu produced by alcohol reduction of the salts. *J. Mater. Res.* 12:398–401
34. Wang W, Chen X, Efrima S. 1999. Silver nanoparticles capped by long chain unsaturated carboxylates. *J. Phys. Chem. B* 103:7238–46
35. Sun Y, Xia Y. 2002. Shape-controlled synthesis of gold and silver nanoparticles. *Science* 298:2176–79
36. Yamamoto M, Nakamoto M. 2003. Novel preparation of monodisperse silver nanoparticles via amine adducts derived from insoluble silver myristate in tertiary alkylamine. *J. Mater. Chem.* 13:2064–65
37. Shen CM, Su YK, Yang HT, Yang TZ, Gao HJ. 2003. Synthesis and characterization of *n*-octadecyl mercaptan-protected palladium nanoparticles. *Chem. Phys. Lett.* 373:39–45
38. Chen S, Huang K, Stearns JA. 2000. Alkanethiolate-protected palladium nanoparticles. *Chem. Mater.* 12:540–47
39. Yee C, Scotti M, Ulman A, White H, Rafailovich M, Sokolov J. 1999. One-phase synthesis of thiol-functionalized platinum nanoparticles. *Langmuir* 15:4314–16
40. Chen S, Kimura K. 2001. Synthesis of thiolate-stabilized nanoparticles in protolytic solvents as isolable colloids. *J. Phys. Chem. B* 105:5397–403
41. Perez H, Pradeau JP, Albouy PA, Perez-Olmil J. 1999. Synthesis and characterization of functionalized platinum nanoparticles. *Chem. Mater.* 11:3460–63
42. Quiros I, Yamada M, Kubo K, Mizutani J, Kurihara M, Nishihara H. 2002. Preparation of alkanethiolate-protected palladium nanoparticles and their size dependence on synthetic conditions. *Langmuir* 18:1413–18
43. Teranishi T, Miyake M. 1998. Size control of palladium nanoparticles and their crystal structures. *Chem. Mater.* 10:594–600
44. Thomas PJ, Kulkarni GU, Rao CNR. 2000. An investigation of two-dimensional arrays of thiolized Pd nanoparticles. *J. Phys. Chem. B* 104:8138–44
45. Mandal S, Selvakannan PR, Roy D, Chaudhari RV, Sastry M. 2002. A new method for the synthesis of hydrophobized, catalytically active Pt nanoparticles. *Chem. Commun.* 24:3002–3
46. Horswell SL, Kiely CJ, O'Neil IA, Schiffrin DJ. 1999. Alkyl isocyanide-derivatized platinum nanoparticles. *J. Am. Chem. Soc.* 121(23):5573–74
47. Alvarez J, Liu J, Roman E, Kaifer AE. 2000. Water-soluble platinum and palladium nanoparticles modified with

- thiolated β -cyclodextrin. *Chem. Commun.* 13:1151–52
48. Kim SW, Park J, Jang Y, Chung Y, Hwang S, et al. 2003. Synthesis of monodisperse palladium nanoparticles. *Nano Lett.* 3:1289–91
 49. Hyeon T. 2003. Chemical synthesis of magnetic nanoparticles. *Chem. Commun.* 8:927–34
 50. Petit C, Taleb A, Pileni MP. 1999. Cobalt nanosized particles organized in a 2D superlattice: synthesis, characterization and magnetic properties. *J. Phys. Chem. B* 103:1805–10
 51. Lin XM, Sorensen CM, Klabunde KJ, Hadjipanayis GC. 1998. Temperature dependence of morphology and magnetic properties of cobalt nanoparticles prepared by an inverse micelle technique. *Langmuir* 14:7140–46
 52. Wilcoxon JP, Provencio PP. 1999. Use of surfactant micelles to control the structural phase of nanosized iron clusters. *J. Phys. Chem. B* 103:9809–12
 53. Suslick KS, Fang M, Hyeon T. 1996. Sonochemical synthesis of iron colloids. *J. Am. Chem. Soc.* 118:11960–61
 54. Suslick KS, Hyeon T, Fang M. 1996. Nanostructured materials generated by high-intensity ultrasound: sonochemical synthesis and catalytic studies. *Chem. Mater.* 8:2172–79
 55. Chen DH, Hsieh CH. 2002. Synthesis of nickel nanoparticles in aqueous cationic surfactant solutions. *J. Mater. Chem.* 12:2412–15
 56. Sun S, Murray CB. 1999. Synthesis of monodisperse cobalt nanocrystals and their assembly into magnetic superlattices. *J. Appl. Phys.* 85:4325–30
 57. Murray CB, Sun S, Gaschler W, Doyle H, Betley TA, Kagan CR. 2001. Colloidal synthesis of nanocrystals and nanocrystal superlattices. *IBM J. Res. Develop.* 45:47–56
 58. Murray CB, Sun S, Doyle H, Betley T. 2001. Monodisperse 3D transition-metal (Co, Ni, Fe) nanoparticles and their assembly into nanoparticle superlattices. *MRS Bull.* 26:985–91
 59. Hou Y, Gao S. 2003. Monodisperse nickel nanoparticles prepared from a monosurfactant system and their magnetic properties. *J. Mater. Chem.* 13:1510–12
 60. Dinega DP, Bawendi MG. 1999. A solution-phase chemical approach to a new crystal structure of cobalt. *Angew. Chem. Int. Ed. Engl.* 38:1788–91
 61. Giersig M, Hilgendorff M. 2002. On the road from single, nanosized magnetic clusters to multi-dimensional nanostructures. *Coll. Surf.* 202:207–13
 62. Puentes VF, Krishnan MK, Alivisatos P. 2001. Synthesis, self-assembly and magnetic behavior of a two-dimensional superlattice of single-crystal ϵ -Co nanoparticles. *App. Phys. Lett.* 78:2187–89
 63. Tripp SL, Pusztay SV, Ribbe AE, Wei A. 2002. Self-assembly of cobalt nanoparticle rings. *J. Am. Chem. Soc.* 124:7914–15
 64. Bonnemann H, Brijoux W, Brinkmann R, Matoussevitch N, Waldofner N, et al. 2003. Size-selective synthesis of air stable colloidal magnetic cobalt nanoparticles. *Inorg. Chim. Acta* 350:617–24
 65. Kim SW, Son SU, Lee SS, Hyeon T, Chung YC. 2001. Colloidal cobalt nanoparticles: a highly active and reusable Pauson-Khand catalyst. *Chem. Commun.* 21:2212–13
 66. Park SJ, Kim S, Lee S, Khim ZG, Char K, Hyeon T. 2000. Synthesis and magnetic studies of uniform iron nanorods and nanospheres. *J. Am. Chem. Soc.* 122:8581–82
 67. Li Y, Liu J, Wang Y, Wang ZL. 2001. Preparation of monodispersed Fe-Mo nanoparticles as the catalyst for CVD synthesis of carbon nanotubes. *Chem. Mater.* 13:1008–14
 68. Sun S, Murray CB, Weller D, Folks L, Moser A. 2000. Monodisperse FePt nanoparticles and ferromagnetic FePt nanocrystal superlattices. *Science* 287:1989–92

69. Sobal NS, Ebels U, Mohwald H, Gierzig M. 2003. Synthesis of core-shell PtCo nanoparticles. *J. Phys. Chem. B* 107: 7351–54
70. Chen M, Nikles DE. 2002. Synthesis of spherical FePd and CoPt nanoparticles. *J. Appl. Phys.* 91:8477–79
71. Osuna J, de Caro D, Amiens C, Chaudret B, Snoeck E, et al. 1996. Synthesis, characterization and magnetic properties of cobalt nanoparticles from an organometallic precursor. *J. Phys. Chem.* 100:14571–74
72. Chen S, Sommers JM. 2001. Alkanethiolate-protected copper nanoparticles: spectroscopy, electrochemistry and solid-state morphological evolution. *J. Phys. Chem. B* 105:8816–20
73. Dhas NA, Raj PC, Gedanken A. 1998. Synthesis, characterisation and properties of metallic copper nanoparticles. *Chem. Mater.* 10:1446–52
74. Lisiecki I, Billoudet F, Pileni MP. 1997. Syntheses of copper nanoparticles in gelified microemulsion and in reverse micelles. *J. Mol. Liq.* 72:251–61
75. Hambrock J, Becker R, Birkner A, Weib J, Fischer RA. 2002. A non-aqueous organometallic route to highly monodisperse copper nanoparticles using $\text{Cu}(\text{OCH}(\text{Me})\text{CH}_2\text{NMe}_2)_2$. *Chem. Commun.* 1:68–69
76. Canham LT. 1990. Silicon quantum wire array fabrication by electrochemical and chemical dissolution of wafers. *Appl. Phys. Lett.* 57(10):1046–48
77. King WD, Boxall DL, Lukehart CM. 1997. Nanoclusters of silicon and germanium. *J. Clust. Sci.* 8(2):267–92
78. Littau KA, Szajowski PJ, Muller AJ, Kortan AR, Brus LE. 1993. A luminescent silicon nanocrystal colloid via a high temperature aerosol reaction. *J. Phys. Chem.* 97:1224–30
79. Ehbrecht M, Kohn B, Huisken F, Laguna MA, Paillard V. 1997. Photoluminescence and resonant Raman spectra of silicon films produced by size-selected cluster beam deposition. *Phys. Rev. B* 56:6958–64
80. Seraphin AA, Werwa E, Kolenbrander KD. 1997. Influence of nanostructure size on the luminescence behavior of silicon nanoparticle thin films. *J. Mater. Res.* 12:3386–92
81. Schuppler S, Friedman SL, Marcus MA, Adler DL, Xie YH, et al. 1994. Dimensions of luminescent oxidized and porous silicon structures. *Phys. Rev. Lett.* 72(16):2648–51
82. Koch F, Petrova-Koch V. 1996. Light from Si-nanoparticle systems—a comprehensive review. *J. Non-Cryst. Solids* 198–200:840–46
83. Paine DC, Caragianis C, Kim TY, Shigesato Y, Ishahara T. 1993. Visible photoluminescence from nanocrystalline Ge formed by H_2 reduction of $\text{Si}_{10.6}\text{Ge}_{0.4}\text{O}_2$. *Appl. Phys. Lett.* 62(22):2842–44
84. Kanemitsu Y, Uto H, Masumoto Y, Maeda Y. 1992. On the origin of visible photoluminescence in nanometer-size Ge crystallites. *Appl. Phys. Lett.* (61):2187–89
85. Venkatasubramanian R, Malta DP, Timmons ML, Hutchby JA. 1991. Visible light emission from quantized planar Ge structures. *Appl. Phys. Lett.* 59(13): 1603–5
86. Wilson WL, Szajowski PF, Brus LE. 1993. Quantum confinement in size-selected, surface oxidized silicon nanocrystals. *Science* 262:1242–44
87. Brus LE, Szajowski PF, Wilson WL, Harris TD, Schuppler S, Citrin PH. 1995. Electron spectroscopy and photophysics of Si nanocrystals: relation to bulk c-Si and porous Si. *J. Am. Chem. Soc.* 117: 2915–22
88. Brus LE. 1994. Luminescence of silicon materials: chains, sheets, nanocrystals, nanowires, microcrystals and porous silicon. *J. Phys. Chem.* 98:3575–81
89. Borsella E, Falconieri M, Botti S, Martelli S, Bignoli F, et al. 2001. Optical and morphological characterization of Si

- nanocrystals/silica composites prepared by sol-gel processing. *Mater. Sci. Eng. B* 79:55–62
90. Botti S, Coppola R, Gourbilleau F, Rizk R. 2000. Photoluminescence from silicon nanoparticles synthesized by laser-induced decomposition of silane. *J. Appl. Phys.* 88(6):3396–401
91. Borsella E, Botti S, Cremona M, Martelli S, Monteleali RM, Nesterenko A. 1997. Photoluminescence from oxidized Si nanoparticles produced by CW CO₂ laser synthesis in a continuous-flow reactor. *J. Mater. Sci. Lett.* 16:221–23
92. Huisken F, Kohn B, Paillard V. 1999. Structured films of light-emitting silicon nanoparticles produced by cluster beam deposition. *Appl. Phys. Lett.* 74(25):3776–78
93. Ledoux G, Gong J, Huisken F. 2001. Effect of passivation and aging on the photoluminescence of silicon nanoparticles. *Appl. Phys. Lett.* 79(24):4028–30
94. Ledoux G, Gong J, Huisken F, Guillois O, Reynaud C. 2002. Photoluminescence of size-separated silicon nanocrystals: confirmation of quantum confinement. *Appl. Phys. Lett.* 80(25):4834–36
95. Li X, He Y, Talukdar SS, Swihart MT. 2003. Process for preparing macroscopic quantities of brightly photoluminescent silicon nanoparticles with emission spanning the visible spectrum. *Langmuir* 19:8490–96
96. Heath JR. 1992. A liquid-solution-phase synthesis of crystalline silicon. *Science* 258:1131–33
97. Heath JR, LeGoues FK. 1993. A liquid solution synthesis of single crystal germanium quantum wires. *Chem. Phys. Lett.* 208(3,4):263–68
98. Kornowski A, Giersig M, Vogel R, Chemseddine A, Weller H. 1993. Nanometer-sized colloidal germanium particles—wet-chemical synthesis, laser-induced crystallization and particle growth. *Adv. Mater.* 5(9):634–36
99. Heath JR, Shiang JJ, Alivisatos PA. 1994. Germanium quantum dots: optical properties and synthesis. *J. Chem. Phys.* 101(2):1607–15
100. Bley RA, Kauzlarich SM. 1996. A low-temperature solution phase route for the synthesis of silicon nanoclusters. *J. Am. Chem. Soc.* 118:12461–62
101. Yang CS, Bley RA, Kauzlarich SM, Lee HWH, Delgado GR. 1999. Synthesis of alkyl-terminated silicon nanoclusters by a solution route. *J. Am. Chem. Soc.* 121:5191–95
102. Mayeri D, Phillips BL, Augustine MP, Kauzlarich SM. 2001. NMR study of the synthesis of alkyl-terminated silicon nanoparticles from the reaction of SiCl₄ with the Zintl salt, NaSi. *Chem. Mater.* 13:765–70
103. Baldwin RK, Pettigrew KA, Ratai E, Augustine MP, Kauzlarich SM. 2002. Solution reduction synthesis of surface stabilized silicon nanoparticles. *Chem. Commun.* 17:1822–23
104. Baldwin RK, Pettigrew KA, Garno JC, Power PP, Liu GY, Kauzlarich SM. 2002. Room temperature solution synthesis of alkyl-capped tetrahedral shaped silicon nanocrystals. *J. Am. Chem. Soc.* 124(7):1150–51
105. Liu Q, Kauzlarich SM. 2002. A new synthetic route for the synthesis of hydrogen terminated silicon nanoparticles. *Mater. Sci. Eng. B* 96:72–75
106. Pettigrew KA, Liu Q, Power PP, Kauzlarich SM. 2003. A new synthetic route to alkyl terminated silicon nanoparticles. *Mat. Res. Soc. Symp. Proc.* 737:F1.8.1–8.6
107. Pettigrew KA, Power PP, Kauzlarich SM. 2003. Solution synthesis of alkyl- and alkyl/alkoxy-capped silicon nanoparticles via oxidation of Mg₂Si. *Chem. Mater.* 15:4005–11
108. Taylor BR, Kauzlarich SM, Lee HWH, Delgado GR. 1998. Solution synthesis of germanium nanocrystals demonstrating quantum confinement. *Chem. Mater.* 10:22–24

109. Taylor BR, Kauzlarich SM, Delgado GR, Lee HWH. 1999. Solution synthesis and characterization of quantum confined Ge nanoparticles. *Chem. Mater.* 11:2493–500
110. Tanke RS, Kauzlarich SM, Patten TE, Pettigrew KA, Murphy DL, et al. 2003. Synthesis of germanium nanoclusters with irreversibly attached functional groups: acetals, alcohols, esters and polymers. *Chem. Mater.* 15:1682–89
111. Ding Z, Quinn BM, Haram SK, Pell LE, Korgel BA, Bard AJ. 2002. Electrochemistry and electrogenerated chemiluminescence from silicon nanocrystal quantum dots. *Science* 296:1293–97
112. Holmes JD, Ziegler KJ, Doty RC, Pell LE, Johnston KP, Korgel BA. 2001. Highly luminescent silicon nanocrystals with discrete optical transitions. *J. Am. Chem. Soc.* 123:3743–48
113. English DS, Pell LE, Yu Z, Barbara PF, Korgel BA. 2002. Size tunable visible luminescence from individual organic monolayer stabilized silicon nanocrystal quantum dots. *Nano Lett.* 2(7):681–85
114. Morales AM, Lieber CM. 1998. A laser ablation method for the synthesis of crystalline semiconductor nanowires. *Science* 279:208–11
115. Lowndes DH, Rouleau CM, Thundat TG, Duscher G, Kenik EA, Pennycook SJ. 1999. Silicon and zinc telluride nanoparticles synthesized by low energy density pulsed laser ablation into ambient gases. *J. Mater. Res.* 14(2):359–69
116. Yoshida T, Yamada Y, Oorii T. 1998. Electroluminescence of silicon nanocrystallites prepared by pulsed laser ablation in reduced pressure inert gas. *J. Appl. Phys.* 83(10):5427–32
117. Carlisle JA, Germanenko IN, Pithawalla YB, El-Shall MS. 2001. Morphology, photoluminescence and electronic structure in oxidized silicon nanoclusters. *J. Electr. Spectr.* 114–116:229–34
118. Seto T, Kawakami Y, Suzuki N, Hirasawa M, Aya N. 2001. Laser synthesis of uniform silicon single nanodots. *Nano Lett.* 1(6):315–18
119. Ngiam ST, Jensen KF, Kolenbrander KD. 1994. Synthesis of Ge nanocrystals embedded in a Si host matrix. *J. Appl. Phys.* 76(12):8201–3
120. Heinrich JL, Curtis CL, Credo GM, Kavanagh KL, Sailor MJ. 1992. Luminescent colloidal silicon suspensions from porous silicon. *Science* 255:66–68
121. Bley RA, Kauzlarich SM, Davis JE, Lee HWH. 1996. Characterization of silicon nanoparticles prepared from porous silicon. *Chem. Mater.* 8:1881–88
122. Kim NY, Laibinis PE. 1997. Thermal derivatization of porous silicon with alcohols. *J. Am. Soc. Chem.* 119:2297–98
123. Dhas NA, Raj CP, Gedanken A. 1998. Preparation of luminescent silicon nanoparticles: a novel sonochemical approach. *Chem. Mater.* 10:3278–81
124. Esteves ACC, Trindade T. 2002. Synthetic studies on II/VI semiconductor quantum dots. *Curr. Opin. Solid State Mater. Sci.* 6(4):347–53
125. Trindade T, O'Brien P, Pickett NL. 2001. Nanocrystalline semiconductors: synthesis, properties, and perspectives. *Chem. Mater.* 13(11):3843–58
126. O'Brien P, Pickett NL. 2004. Strategies for the scalable synthesis of quantum dots and related nanodimensional materials. See Ref. 264. In press
127. Peng X. 2002. Green chemical approaches toward high-quality semiconductor nanocrystals. *Chem. Eur. J.* 8(2): 335–39
128. Brus LE. 1984. Electron-electron and electron-hole interactions in small semiconductor crystallites: the size dependence of the lowest excited electronic state. *J. Chem. Phys.* 80(9):4403–9
129. Rossetti R, Ellison JL, Gibson JM, Brus LE. 1984. Size effects in the excited electronic states of small colloidal CdS crystallites. *J. Chem. Phys.* 80(9):4464–69
130. Rossetti R, Hull R, Gibson JM, Brus LE. 1985. Excited electronic states and optical

- spectra of ZnS and CdS crystallites in the ≈ 15 to 50 Å size range: evolution from molecular to bulk semiconducting properties. *J. Chem. Phys.* 82(1):552–59
131. Rogach AL, Kornowski A, Gao M, Eychmüller A, Weller H. 1999. Synthesis and characterization of a size series of extremely small thiol-stabilized CdSe nanocrystals. *J. Phys. Chem. B* 103:3065–69
132. Rogach A, Kershaw S, Burt M, Harrison M, Kornowski A, et al. 1999. Colloidally prepared HgTe nanocrystals with strong room-temperature infrared luminescence. *Adv. Mater.* 11(7):552–55
133. Harrison MT, Kershaw SV, Burt MG, Eychmüller A, Weller H, Rogach AL. 2000. Wet chemical synthesis and spectroscopic study of CdHgTe nanocrystals with strong near-infrared luminescence. *Mater. Sci. Eng. B* 69–70:355–60
134. Spanhel L, Haase M, Weller H, Henglein A. 1987. Photochemistry of colloidal semiconductors. Surface modification and stability of strong luminescing CdS particles. *J. Am. Chem. Soc.* 109: 5649–55
135. Gaponik N, Talapin DV, Rogach AL, Hoppe K, Shevchenko EV, et al. 2002. Thiol-capping of CdTe nanocrystals: an alternative to organometallic synthetic routes. *J. Phys. Chem. B* 106:7177–85
136. Vossmeier T, Katsikas L, Giersig M, Popovic IG, Diesner K, et al. 1994. CdS nanoclusters: synthesis, characterization, size dependent oscillator strength, temperature shift of the excitonic transition energy, and reversible absorbance shift. *J. Phys. Chem.* 98:7665–73
137. Wang W, Germanenko I, El-Shall MS. 2002. Room-temperature synthesis and characterization of nanocrystalline CdS, ZnS and $Cd_xZn_{1-x}S$. *Chem. Mater.* 14: 3028–33
138. Wang W, Geng Y, Yan P, Liu F, Xie Y, Qian Y. 1999. A novel mild route to nanocrystalline selenides at room temperature. *J. Am. Chem. Soc.* 121:4062–63
139. Lifshitz E, Bashouti M, Kloper V, Kigel A, Eisen MS, Berger S. 2003. Synthesis and characterization of PbSe quantum wires, multipods, quantum rods, and cubes. *Nano Lett.* 3(6):857–62
140. Mastai Y, Polsky R, Koltypin Y, Gedanken A, Hodes G. 1999. Pulsed sonoelectrochemical synthesis of cadmium selenide nanoparticles. *J. Am. Chem. Soc.* 121:10047–52
141. Zhu J, Aruna ST, Koltypin Y, Gedanken A. 2000. A novel method for the preparation of lead selenide: pulse sonoelectrochemical synthesis of lead selenide nanoparticles. *Chem. Mater.* 12:143–47
142. Zhu J, Koltypin Y, Gedanken A. 2000. General sonochemical method for the preparation of nanophasic selenides: synthesis of ZnSe nanoparticles. *Chem. Mater.* 12:73–78
143. Murray CB, Norris DJ, Bawendi MG. 1993. Synthesis and characterization of nearly monodisperse CdE (E = S, Se, Te) semiconductor nanocrystallites. *J. Am. Chem. Soc.* 115:8706–15
144. Alivisatos PA. 1996. Perspectives on the physical chemistry of semiconductor nanocrystals. *J. Phys. Chem.* 100:13226–39
145. Manna L, Scher EC, Alivisatos PA. 2000. Synthesis of soluble and processable rod-, arrow-, teardrop-, and tetrapod-shaped CdSe nanocrystals. *J. Am. Chem. Soc.* 122(51):12700–6
146. Peng X, Manna L, Yang W, Wickham J, Scher E, et al. 2000. Shape control of CdSe nanocrystals. *Nature* 404(2):59–61
147. Peng X, Wickham J, Alivisatos AP. 1998. Kinetics of II–VI and III–V colloidal semiconductor nanocrystal growth: “focusing” of size distributions. *J. Am. Chem. Soc.* 120:5343–44
148. Hines MA, Guyot-Sionnest P. 1996. Synthesis and characterization of strongly luminescing ZnS-capped CdSe nanocrystals. *J. Phys. Chem.* 100:468–71
149. Danek M, Jensen KF, Murray CB, Bawendi MG. 1996. Synthesis of

- luminescent thin film CdSe/ZnSe quantum dot composites using CdSe quantum dots passivated with an overlayer of ZnSe. *Chem. Mater.* 8:173–80
150. Dabbousi BO, Rodriguez-Viejo J, Mikulec FV, Heine JR, Mattoussi H, et al. 1997. (CdSe)ZnS core-shell quantum dots: synthesis and characterization of a size series of highly luminescent nanocrystallites. *J. Phys. Chem. B* 101:9463–75
151. Peng X, Schlamp MC, Kadavanich AV, Alivisatos AP. 1997. Epitaxial growth of highly luminescent CdSe/CdS core/shell nanocrystals with photostability and electronic accessibility. *J. Am. Chem. Soc.* 119:7019–29
152. Rajeshwar K, de Tacconi NR, Chenthamarakshan CR. 2001. Semiconductor-based composite materials: preparation, properties, and performance. *Chem. Mater.* 13(9):2765–82
153. Eychmüller A. 2000. Structure and photophysics of semiconductor nanocrystals. *J. Phys. Chem. B* 104(28):6514–28
154. Peng ZA, Peng X. 2001. Formation of high-quality CdTe, CdSe, and CdS nanocrystals using CdO as precursor. *J. Am. Chem. Soc.* 123:183–84
155. Qu L, Peng ZA, Peng X. 2001. Alternative routes toward high quality CdSe nanocrystals. *Nano Lett.* 1(6):333–37
156. Peng ZA, Peng X. 2001. Mechanisms of the shape evolution of CdSe nanocrystals. *J. Am. Chem. Soc.* 123:1389–95
157. Peng ZA, Peng X. 2002. Nearly monodisperse and shape-controlled CdSe nanocrystals via alternative routes: nucleation and growth. *J. Am. Chem. Soc.* 124:3343–53
158. Manna L, Milliron DJ, Meisel A, Scher E, Alivisatos AP. 2003. Controlled growth of tetrapod-branched inorganic nanocrystals. *Nature Mater.* 2:382–85
159. Brennan JG, Siegrist T, Carroll PJ, Stuczynski SM, Brus LE, Steigerwald ML. 1989. The preparation of large semiconductor clusters via the pyrolysis of a molecular precursor. *J. Am. Chem. Soc.* 111:4141–43
160. Pickett NL, O'Brien P. 2001. Syntheses of semiconductor nanoparticles using single-molecular precursors. *Chem. Rec.* 1:467–79
161. Malik MA, O'Brien P, Revaprasadu N. 2002. A simple route to the synthesis of core/shell nanoparticles of chalcogenides. *Chem. Mater.* 14(5):2004–10
162. Revaprasadu N, Malik MA, O'Brien P, Wakefield G. 1999. Deposition of zinc sulfide quantum dots from a single-source molecular precursor. *J. Mater. Res.* 14(8):3237–40
163. Revaprasadu N, Malik MA, O'Brien P, Zulu MM, Wakefield G. 1998. Single-source molecular precursor for the deposition of zinc selenide quantum dots. *J. Mater. Chem.* 8(8):1885–88
164. Trindade T, O'Brien P, Zhang X. 1997. Synthesis of CdS and CdSe nanocrystallites using a novel single-molecule precursors approach. *Chem. Mater.* 9:523–30
165. Ludolph B, Malik MA, O'Brien P, Revaprasadu N. 1998. Novel single molecule precursor routes for the direct synthesis of highly monodispersed quantum dots of cadmium or zinc sulfide or selenide. *Chem. Commun.* 17:1849–50
166. Revaprasadu N, Malik MA, O'Brien P, Wakefield G. 1999. A simple route to synthesize nanodimensional CdSe-CdS core-shell structures from single molecular precursors. *Chem. Commun.* 16:1573–74
167. Lazell M, O'Brien P. 1999. A novel single source precursor route to self capping CdS quantum dots. *Chem. Commun.* 20:2041–42
168. Trindade T, Monteiro OC, O'Brien P, Motevalli M. 1999. Synthesis of PbSe nanocrystallites using a single-source method. The X-ray crystal structure of lead(II) diethyldiselenocarbamate. *Polyhedron* 18:1171–75
169. Trindade T, O'Brien P, Zhang X, Motevalli M. 1997. Synthesis of PbS nanocrystallites using a novel single molecule

- precursors approach: X-ray single-crystal structure of $\text{Pb}(\text{S}_2\text{CNEtPr}^f)_2$. *J. Mater. Chem.* 7(6):1011–16
170. Jun YW, Lee SM, Kang NJ, Cheon J. 2001. Controlled synthesis of multi-armed CdS nanorod architectures using monosurfactant system. *J. Am. Chem. Soc.* 123:5150–51
171. Malik MA, Revaprasadu N, O'Brien P. 2001. Air-stable single-source precursors for the synthesis of chalcogenide semiconductor nanoparticles. *Chem. Mater.* 13(3):913–20
172. Nair PS, Radhakrishnan T, Revaprasadu N, Kolawole GA, O'Brien P. 2002. A single-source route to CdS nanorods. *Chem. Commun.* 6:564–65
173. Crouch DJ, O'Brien P, Malik MA, Skabarara PJ, Wright SP. 2003. A one-step synthesis of cadmium selenide quantum dots from a novel single source precursor. *Chem. Commun.* 12:1454–55
174. Nair PS, Radhakrishnan T, Revaprasadu N, Kolawole GA, O'Brien P. 2003. $\text{Cd}(\text{NH}_2\text{CSNHNHCSNH}_2)\text{Cl}_2$: a new single-source precursor for the preparation of CdS nanoparticles. *Polyhedron* 22(23):3129–35
175. Nair PS, Radhakrishnan T, Revaprasadu N, Kolawole GA, O'Brien P. 2002. Cadmium ethylxanthate: a novel single-source precursor for the preparation of CdS nanoparticles. *J. Mater. Chem.* 12(9):2722–25
176. Dance IG, Choy A, Schudder ML. 1984. Syntheses, properties, and molecular and crystal structures of $(\text{Me}_4\text{N})_4[\text{E}_4\text{M}_{10}(\text{SPh})_{16}]$ ($\text{E} = \text{S}, \text{Se}; \text{M} = \text{Zn}, \text{Cd}$): molecular supertetrahedral fragments of the cubic metal chalcogenide lattice. *J. Am. Chem. Soc.* 106:6285–95
177. Cumberland SL, Hanif KM, Javier A, Khitrov GA, Strouse GF, et al. 2002. Inorganic clusters as single-source precursors for preparation of CdSe, ZnSe, and CdSe/ZnS nanomaterials. *Chem. Mater.* 14:1576–84
178. Byrappa K, Yoshimura M. 2001. *Handbook of Hydrothermal Technology*. Norwich, New York: William Andrew Publ.
179. Li Y, Ding Y, Qian Y, Zhang Y, Yang L. 1998. A solvothermal elemental reaction to produce nanocrystalline ZnSe. *Inorg. Chem.* 37:2844–45
180. Peng Q, Dong Y, Deng Z, Sun X, Li Y. 2001. Low-temperature elemental-direct-reaction route to II–VI semiconductor nanocrystalline ZnSe and CdSe. *Inorg. Chem.* 40:3840–41
181. Zhan JH, Yang XG, Zhang WX, Wang DW, Xie Y, Qian YT. 2000. A solvothermal route to wurzite ZnSe nanoparticles. *J. Mater. Res.* 15:629–32
182. Deng ZX, Wang C, Sun MX, Li DY. 2002. Structure-directing coordination template effect of ethylenediamine in formations of ZnS and ZnSe nanocrystallites via solvothermal route. *Inorg. Chem.* 41(4):869–73
183. Yu SH, Wu YS, Yang J, Han ZH, Xie Y, et al. 1998. A novel solventothermal synthetic route to nanocrystalline CdE ($\text{E} = \text{S}, \text{Se}, \text{Te}$) and morphological control. *Chem. Mater.* 10:2309–12
184. Yu SH, Yang J, Han ZH, Zhou Y, Yang RY, et al. 1999. Controllable synthesis of nanocrystalline CdS with different morphologies and particle sizes by a novel solvothermal process. *J. Mater. Chem.* 9:1283–87
185. Gautam UK, Rajamathi M, Meldrum F, Morgan P, Seshadri R. 2001. A solvothermal route to capped CdSe nanoparticles. *Chem. Commun.* 7:629–30
186. Gautam UK, Seshadri R, Rao CNR. 2003. A solvothermal route to CdS nanocrystals. *Chem. Phys. Lett.* 375:560–64
187. Heath JR, Shiang JJ. 1998. Covalency in semiconductor quantum dots. *Chem. Soc. Rev.* 27(1):65–71
188. Green M, O'Brien P. 1999. Recent advances in the preparation of semiconductors as isolated nanometric particles: new routes to quantum dots. *Chem. Commun.* 22:2235–41

189. Green M. 2002. Solution routes to III–V semiconductor quantum dots. *Curr. Opin. Solid State Mater. Sci.* 6:355–63
190. Wells RL, Pitt CG, McPhail AT, Purdy AP, Shafieezad S, Hallock RB. 1989. Use of tris(trimethylsilyl)arsine to prepare gallium arsenide and indium arsenide. *Chem. Mater.* 1:4–6
191. Wells RL, Hallock RB, McPhail AT, Pitt CG, Johansen JD. 1991. Preparation of a novel gallium arsenide single-source precursor having the empirical formula AsCl_3Ga_2 . *Chem. Mater.* 3:381–82
192. Wells RL, Aubuchon SR, Kher SS, Lube MS, White PS. 1995. Synthesis of nanocrystalline indium arsenide and indium phosphide from indium(III) halides and tris(trimethylsilyl)pnictogens. Synthesis, characterization, and decomposition behavior of $\text{I}_3\text{InP}(\text{SiMe}_3)_3$. *Chem. Mater.* 7:793–800
193. Olshavsky MA, Goldstein AN, Alivisatos AP. 1990. Organometallic synthesis of GaAs crystallites exhibiting quantum confinement. *J. Am. Chem. Soc.* 112: 9438–39
194. Uchida H, Curtis CJ, Nozik AJ. 1991. GaAs nanocrystals prepared in quinoline. *J. Phys. Chem.* 95:5382–84
195. Uchida H, Curtis CJ, Kamat PV, Jones KM, Nozik AJ. 1992. Optical properties of GaAs nanocrystals. *J. Phys. Chem.* 96:1156–60
196. Guzelian AA, Katari JEB, Kadavanich AV, Banin U, Hamad K, et al. 1996. Synthesis of size-selected, surface-passivated InP nanocrystals. *J. Phys. Chem.* 100:7212–19
197. Guzelian AA, Banin U, Kadavanich AV, Peng X, Alivisatos AP. 1996. Colloidal chemical synthesis and characterization of InAs nanocrystal quantum dots. *Appl. Phys. Lett.* 69(10):1432–34
198. Mičić OI, Curtis CJ, Jones KM, Sprague JR, Nozik AJ. 1994. Synthesis and characterization of InP quantum dots. *J. Phys. Chem.* 98:4966–69
199. Mičić OI, Sprague JR, Curtis CJ, Jones KM, Machol JL, et al. 1995. Synthesis and characterization of InP, GaP, and GaInP_2 quantum dots. *J. Phys. Chem.* 99:7754–59
200. Mičić OI, Ahrenkiel SP, Nozik AJ. 2001. Synthesis of extremely small InP quantum dots and electronic coupling in their disordered solid films. *Appl. Phys. Lett.* 78(25):4022–24
201. Malik MA, O'Brien P, Norager S, Smith J. 2003. Gallium arsenide nanoparticles: synthesis and characterization. *J. Mater. Chem.* 13:2591–95
202. Wells RL, Self MF, McPhail AT, Aubuchon SR, Woudenberg RC, Jasiniski JP. 1993. Synthesis, characterization, and thermal decomposition of $[\text{Cl}_2\text{GaP}(\text{SiMe}_3)_2]_2$, a potential precursor to gallium phosphide. *Organometallics* 12:2832–34
203. Battaglia D, Peng X. 2002. Formation of high quality InP and InAs nanocrystals in a non-coordinating solvent. *Nano Lett.* 2(9):1027–30
204. Cao YW, Banin U. 1999. Synthesis and characterization of InAs/InP and InAs/CdSe core/shell nanocrystals. *Angew. Chem. Int. Ed. Engl.* 38(24):3692–94
205. Cao YW, Banin U. 2000. Growth and properties of semiconductor core/shell nanocrystals with InAs cores. *J. Am. Chem. Soc.* 122:9692–702
206. Green M, O'Brien P. 1998. A novel metalorganic route for the direct and rapid synthesis of monodispersed quantum dots of indium phosphide. *Chem. Commun.* (22):2459–60
207. Janik JF, Wells RL, Young VG, Rheingold AL, Guzei IA. 1998. New pnictinogallanes $[\text{H}_2\text{GaE}(\text{SiMe}_3)_2]_3$ (E = P, As)—formation, structural characterization, and thermal decomposition to afford nanocrystalline GaP and GaAs. *J. Am. Chem. Soc.* 120(3):532–37
208. Kher SS, Wells RL. 1994. A straightforward, new method for the synthesis of nanocrystalline GaAs and GaP. *Chem. Mater.* 6:2056–62

209. Gao S, Lu J, Chen N, Zhao Y, Xie Y. 2002. Aqueous synthesis of III–V semiconductor GaP and InP exhibiting pronounced quantum confinement. *Chem. Commun.* 24:3064–65
210. Gao S, Lu J, Zhan Y, Chen N, Xie Y. 2002. Thermic conversion of benzene into 6-phenylfulvene with high yield mediated by GaP nanocrystals. *Chem. Commun.* 23:2880–81
211. Qian YT. 1999. Solvothermal synthesis of nanocrystalline III–V semiconductors. *Adv. Mater.* 11(13):1101–2
212. Li DY, Duan XF, Qian YT, Yang L, Ji MR, Li CW. 1997. Solvothermal co-reduction route to the nanocrystalline III–V semiconductor InAs. *J. Am. Chem. Soc.* 119:7869–70
213. Xie Y, Qian YT, Wang W, Zhang S, Zhang Y. 1996. A benzene-thermal synthetic route to nanocrystalline GaN. *Science* 272:1926–27
214. Rao CNR. 1989. Transition metal oxides. *Annu. Rev. Phys. Chem.* 40:291–326
215. Rajamathi M, Seshadri R. 2002. Oxide and chalcogenide nanoparticles from hydrothermal/solvothermal reactions. *Curr. Opin. Solid State Mater. Sci.* 6:337–45
216. Seshadri R. 2004. Oxide nanoparticles. See Ref. 264. In press
217. Blakemore R. 1975. Magnetotactic bacteria. *Science* 190:377–79
218. Frankel RB, Blakemore RP, Wolfe RS. 1979. Magnetite in freshwater magnetotactic bacteria. *Science* 203:1355–56
219. Dunin-Borkowski RE, McCartney MR, Frankel RB, Bazylinski DA, Pósfai M, Buseck PR. 1998. Magnetic microstructure of magnetotactic bacteria by electron holography. *Science* 282:1868–70
220. Cabuil V. 2000. Phase behavior of magnetic nanoparticles dispersions in bulk and confined geometries. *Curr. Opin. Colloid Interface Sci.* 5:44–48
221. Chen JP, Sorenson CM, Klabunde KJ, Hadjipanayis GC, Devlin E, Kostikas A. 1996. Size-dependent magnetic properties of MnFe₂O₄ fine particles synthesized by coprecipitation. *Phys. Rev. B* 54:9288–96
222. Lefebure S, Dubois E, Cabuil V, Neveu S, Massart R. 1998. Monodisperse magnetic nanoparticles: preparation and dispersion in water and oils. *J. Mater. Res.* 13:2975–81
223. Massart R, Dubois E, Cabuil V, Hasmonay E. 1995. Preparation and properties of monodisperse magnetic fluids. *J. Magn. Magn. Mater.* 149:1–5
224. Morales MP, Veintemillas-Verdaguer S, Montero MI, Serna CJ, Roig A, et al. 1999. Surface and internal spin canting in γ -Fe₂O₃ nanoparticles. *Chem. Mater.* 11:3058–64
225. Ammar S, Helfen A, Jouini N, Fiévet F, Rosenman I, et al. 2001. Magnetic properties of ultrafine cobalt ferrite particles synthesized by hydrolysis in a polyol medium. *J. Mater. Chem.* 11:186–92
226. Rajamathi M, Ghosh M, Seshadri R. 2002. Hydrolysis and amine-capping in a glycol solvent as a route to soluble maghemite γ -Fe₂O₃ nanoparticles. *Chem. Commun.* 10:1152–53
227. Caruntu D, Remond Y, Chou N-H, Jun M-J, Caruntu G, et al. 2002. Reactivity of 3D transition metal cations in diethylene glycol solutions. Synthesis of transition metal ferrites with the structure of discrete nanoparticles complexed with long-chain carboxylate anions. *Inorg. Chem.* 41:6137–46
228. Pileni MP. 1997. Reverse micelles as microreactors. *J. Phys. Chem.* 97:6961–73
229. Pileni MP. 1993. Nanosized particles made in colloidal assemblies. *Langmuir* 13:3266–76
230. Pillai V, Shah DO. 1996. Synthesis of high-coercivity cobalt ferrite particles using water-in-oil microemulsions. *J. Magn. Magn. Mater.* 163:243–48
231. Liu C, Zhang ZJ. 2001. Size-dependent superparamagnetic properties of Mn spinel ferrite nanoparticles synthesized

- from reverse micelles. *Chem. Mater.* 13: 2092–96
232. Vestal CR, Zhang ZJ. 2002. Synthesis of CoCrFeO_4 nanoparticles using microemulsion methods and size-dependent studies of their magnetic properties. *Chem. Mater.* 14:3817–22
233. Moumen N, Pileni MP. 1996. New syntheses of cobalt ferrite particles in the range 2–5 nm: comparison of the magnetic properties of the nanosized particles in dispersed fluid or in powder form. *Chem. Mater.* 8:1128–34
234. Moumen N, Pileni MP. 1996. Control of the size of cobalt ferrite magnetic fluid. *J. Phys. Chem.* 100:1867–73
235. Moumen N, Bonville P, Pileni MP. 1996. Control of the size of cobalt ferrite magnetic fluids: Mössbauer spectroscopy. *J. Phys. Chem.* 100:14410–16
236. Hochepped JF, Sainctavit Ph, Pileni MP. 2001. X-ray absorption spectra and X-ray magnetic circular dichroism studies at Fe and Co $L_{2,3}$ edges of mixed cobalt-zinc ferrite nanoparticles: cationic repartition, magnetic structure and hysteresis cycles. *J. Magn. Magn. Mater.* 231:315–22
237. Hochepped JF, Bonville P, Pileni MP. 2000. Nonstoichiometric zinc ferrite nanocrystals: syntheses and unusual magnetic properties. *J. Phys. Chem. B* 104: 905–12
238. Ngo AT, Pileni MP. 2001. Assemblies of ferrite nanocrystals: partial orientation of the easy magnetic axes. *J. Phys. Chem. B* 105:53–58
239. Vijaya Kumar R, Diamant Y, Gedanken A. 2000. Sonochemical synthesis and characterization of nanometer-size transition metal oxides from metal acetates. *Chem. Mater.* 12:2301–5
240. Vijaya Kumar R, Koltypin Y, Xu XN, Yeshurun Y, Gedanken A, Felner I. 2001. Fabrication of magnetite nanorods by ultrasound irradiation. *J. Appl. Phys.* 89: 6324–28
241. Bentzon MD, van Wonterghem J, Mørup S, Thölén A. 1989. Ordered aggregates of ultrafine iron oxide particles—supercrystals. *Phil. Mag. B* 60:169–78
242. Hyeon T, Lee SS, Park J, Chung Y, Na HB. 2001. Synthesis of highly crystalline and monodisperse maghemite nanocrystallites without a size-selection process. *J. Am. Chem. Soc.* 123:12798–801
243. Hyeon T, Chung Y, Park J, Lee SS, Kim Y-W, Park BH. 2002. Synthesis of highly crystalline and monodisperse cobalt ferrite nanocrystals. *J. Phys. Chem. B* 106:6831–33
244. Nelson JA, Wagner MJ. 2002. Yttrium oxide nanoparticles prepared by alkali reduction. *Chem. Mater.* 14:915–17
245. Nelson JA, Brant EL, Wagner MJ. 2003. Nanocrystalline Y_2O_3 :Eu phosphors prepared by alkali reduction. *Chem. Mater.* 15:688–93
246. Rockenberger J, Scher EC, Alivisatos AP. 1999. A new nonhydrolytic single-precursor approach to surfactant-capped nanocrystals of transition metal oxides. *J. Am. Chem. Soc.* 121:11595–96
247. Boal AK, Das K, Gray M, Rotello VM. 2002. Monolayer exchange chemistry of $\gamma\text{-Fe}_2\text{O}_3$ nanoparticles. *Chem. Mater.* 14:2628–36
248. Bourlinos AB, Simopoulos A, Petrides D. 2002. Synthesis of capped ultrafine $\gamma\text{-Fe}_2\text{O}_3$ particles from iron(III) hydroxide caprylate: a novel starting material for readily attainable organosols. *Chem. Mater.* 14:899–903
249. Bourlinos AB, Bakandritsos A, Georgakilas V, Petrides D. 2002. Surface modification of ultrafine magnetic iron oxide particles. *Chem. Mater.* 14:3226–28
250. O'Brien S, Brus L, Murray CB. 2001. Synthesis of monodisperse nanoparticles of barium titanate: Toward a generalized strategy of oxide nanoparticle synthesis. *J. Am. Chem. Soc.* 123:12085–86
251. Arnal P, Corriu RJP, Leclercq D, Mutin PH, Vioux A. 1997. A solution chemistry study of nonhydrolytic sol-gel routes to titania. *Chem. Mater.* 9:694–98

252. Trentler TJ, Denler TE, Bertone JF, Agrawal A, Colvin VL. 1999. Synthesis of TiO₂ nanocrystals by nonhydrolytic solution-based reactions. *J. Am. Chem. Soc.* 121:1613–14
253. Joo J, Yu T, Kim YW, Park HM, Wu F, et al. 2003. Multigram scale synthesis and characterization of monodisperse tetragonal zirconia nanocrystals. *J. Am. Chem. Soc.* 125:6553–57
254. Inoue M, Kimura M, Inui T. 1999. Transparent colloidal solution of 2 nm ceria particles. *Chem. Commun.* 11:957–58
255. Li Y, Duan X, Liao H, Qian Y. 1998. Self-regulation synthesis of nanocrystalline ZnGa₂O₄ by hydrothermal reaction. *Chem. Mater.* 10:17–18
256. Chemseddine A, Moritz T. 1999. Nanostructuring titania: control over nanocrystal structure, size, shape and organization. *Eur. J. Inorg. Chem.* 2:235–245
257. Wu M, Long J, Huang A, Luo Y, Feng S, Xu R. 1999. Microemulsion-mediated hydrothermal synthesis and characterization of nanosize rutile and anatase particles. *Langmuir* 15:8822–25
258. Hirano M. 2000. Hydrothermal synthesis and characterization of ZnGa₂O₄ spinel fine particles. *J. Mater. Chem.* 10:469–72
259. Cabañas A, Darr JA, Lester E, Poliakov M. 2000. A continuous and clean one-step synthesis of nano-particulate Ce_{1-x}Zr_xO₂ solid solutions in near-critical water. *Chem. Commun.* 11:901–2
260. Cabañas A, Darr JA, Lester E, Poliakov M. 2001. Continuous hydrothermal synthesis of inorganic materials in a near-critical water flow reactor; the one-step synthesis of nano-particulate Ce_{1-x}Zr_xO₂ (x = 0–1) solid solutions. *J. Mater. Chem.* 11:561–68
261. LaMer VK, Dinegar RH. 1950. Theory, production and mechanism of formation of monodispersed hydrosols. *J. Am. Chem. Soc.* 72:4847–54
262. Cabañas A, Poliakov M. 2001. The continuous hydrothermal synthesis of nano-particulate ferrites in near critical and supercritical water. *J. Mater. Chem.* 11:1408–16
263. Thimmaiah S, Rajamathi M, Singh N, Bera P, Meldrum F, et al. 2001. A solvothermal route to capped nanoparticles of γ -Fe₂O₃ and CoFe₂O₄. *J. Mater. Chem.* 11:3215–21
264. Rao CNR, Müller A, Cheetham AK, eds. 2004. *The Chemistry of Nanomaterials: Synthesis, Properties, and Applications*. Weinheim: Wiley-VCH

Copyright of Annual Review of Materials Research is the property of Annual Reviews Inc. and its content may not be copied or emailed to multiple sites or posted to a listserv without the copyright holder's express written permission. However, users may print, download, or email articles for individual use.